

**Universidade de Lisboa  
Faculdade de Ciências  
Departamento de Biologia Vegetal**



**Digested raspberries polyphenols for brain health:  
Attenuation of neuroinflammation**

Gonçalo Filipe Rodrigues Garcia

**Dissertação**

**Mestrado em Biologia Molecular e Genética**

**2014**

**Universidade de Lisboa  
Faculdade de Ciências  
Departamento de Biologia Vegetal**



**Digested raspberries polyphenols for brain health:  
Attenuation of neuroinflammation**

**Gonçalo Filipe Rodrigues Garcia**

**Sob a orientação de:**

Maria Helena Caria, PhD  
(Prof. Auxiliar FCUL; Prof. Coordenadora ESS-IPS)  
Maria Paula Marinho Pinto, PhD  
(Investigadora convidada ITQB; Prof. Coordenadora ESA-IPS)

**Dissertação**

**Mestrado em Biologia Molecular e Genética**

**2014**

## *Epigraph*

“Sage isn't the man who gives the true answers;  
is the one who formulates the true questions”

**Claude Lévi-Strauss**

## *Acknowledgments*

I would like to start by expressing my acknowledgement to Maria Paula Marinho Pinto, my supervisor. My gratitude for all the support, guidance and encouragement given during this incredibly intensive year. Also, Cláudia Nunes dos Santos, who gave me alternatives to the problems and always helped me to clarify and rethink the way how I was working. Thanks to both, who always had patience to listen to me, always with willingness.

My special thanks go also to Professor Ricardo Boavida Ferreira, who allowed my inclusion in the workgroup at his laboratory. Thanks for the opportunity, and for all the knowledge and experience. A note of thanks is also due to Dr. Teresa Pais (IMM, Lisbon), and Dr. Derek Stewart (JHI, Dundee) who, respectively, provided the N9 microglial cell line and the five quasi-isogenic digested raspberry polyphenolic fractions I used at this work. I would like to express my appreciation to Dr. Regina Menezes, especially for introducing me to the yeast model of neuroinflammation, but also for the critical reading of this thesis, providing numerous suggestions for its improvement. Additionally, my sincere thanks to Dr. Maria Helena Caria for having accepted to be my supervisor and for the support offered during all my work.

I cannot forget all my Disease and Stress Biology laboratory colleagues, who had a critical role in my progress over the year. Thanks to Andreia Gomes for her hospitality and readiness to help; to Carolina Jardim for her friendly disposition and comprehension; to Lucélia Tavares for her good and wise advices; to Inês Figueira for her authenticity and critical rigor; to Rui Pimpão for sharing his experience and social skills. Without them, I would not know how hard it is the world of science. You gave me strength. Thank you for all the time spent discussing results, for all the encouragement and support.

A very special acknowledge goes to the other trainees, who also started their stages at the same time as I did. Many thanks to Tânia Silva for sharing great moments in the laboratory, and for her good humor; to Vitor Hugo Gonçalves for being my laboratory brother, and for all the jokes and comprehension given; to Inês Costa for being always an exceptional person and an example in the organization and work. All of you were part my closest family during the past year, many thanks. I will never forget all the moments we spent together.

Also, I want to thank my family. To my parents and brother, without them would be impossible to keep studying and reaching my objectives. Many thanks! To Carmen Santos who had a crucial role in my stage since the beginning, when I had many doubts about what I would like to do during the year. Thanks for all the discussions we made about this thesis and the practical work; and many thanks for your comprehension and sensitive capacity. To Daniel Gaspar, my “praxis brother”, who distracted me when necessary, always providing a good company. Many thanks to all of you!!

# Index

INDEX .....	V
INDEX OF FIGURES.....	VI
INDEX OF TABLES.....	VI
ABBREVIATIONS.....	VII
ABSTRACT .....	IX
<b>KEYWORDS</b> .....	<b>IX</b>
RESUMO.....	X
<b>PALAVRAS-CHAVE</b> .....	<b>XII</b>
1.    OBJECTIVES .....	1
2.    THEORETICAL FUNDAMENTS.....	2
<b>2.1. MICROGLIA: THE INNATE IMMUNE CELL OF CENTRAL NERVOUS SYSTEM</b> .....	<b>2</b>
<b>2.2. NEUROINFLAMMATION</b> .....	<b>3</b>
<b>2.2.1 – Markers of microglial activation</b> .....	<b>4</b>
<b>2.2.2 – Common Inflammatory triggers</b> .....	<b>8</b>
<b>2.3. ATTENUATION OF NEUROINFLAMMATION BY DIETARY FACTORS</b> .....	<b>8</b>
<b>2.3.1 – Attenuation of neuroinflammation by polyphenols</b> .....	<b>9</b>
<b>2.3.2 – Polyphenols metabolites</b> .....	<b>10</b>
<b>2.3.3 - Raspberry: a fruit with potential anti-neuroinflammatory properties</b> .....	<b>10</b>
3. MATERIALS AND METHODS.....	12
<b>3.1. PLANT MATERIAL, IN VITRO DIGESTION AND FRACTIONS PREPARATION</b> .....	<b>12</b>
<b>3.2. MICROGLIAL MODEL OF NEUROINFLAMMATION</b> .....	<b>13</b>
<b>3.2.1 – Cell culture and treatments</b> .....	<b>13</b>
<b>3.2.2 – Protein extraction and quantification</b> .....	<b>13</b>
<b>3.2.3 – Determination of pro-inflammatory and activation markers</b> .....	<b>14</b>
<b>3.2.4 – Cytotoxicity assays</b> .....	<b>16</b>
<b>3.3. YEAST MODEL OF INFLAMMATION</b> .....	<b>16</b>
<b>3.3.1. Characterization of <i>S. cerevisiae</i> model of inflammation</b> .....	<b>16</b>
<b>3.3.2 – <math>\beta</math>-galactosidase assays</b> .....	<b>17</b>
<b>3.4. STATISTICS</b> .....	<b>18</b>
4. RESULTS AND DISCUSSION .....	19
<b>4.1. ATTENUATION OF NEUROINFLAMMATION IN MURINE MICROGLIAL CELL LINE N9</b> .....	<b>19</b>
<b>4.1.1 – Implementation of N9 microglial line as a neuroinflammation model</b> .....	<b>19</b>
<b>4.1.2 – Cytotoxicity of the digested raspberry polyphenolic fractions</b> .....	<b>21</b>
<b>4.1.3 – Model optimization for attenuation of neuroinflammation</b> .....	<b>22</b>
<b>4.1.4 – Attenuation of neuroinflammation by raspberry digested fractions</b> .....	<b>23</b>
<b>4.2. MECHANISTIC STUDIES OF ANTI-INFLAMMATORY PROPERTIES OF DIGESTED RASPBERRY POLYPHENOLS IN SACCHAROMYCES CEREVISIAE MODELS</b> .....	<b>25</b>
<b>4.2.1 – Digested raspberry polyphenols modulate the <i>Crz1</i>/calcineurin pathway</b> .....	<b>25</b>
5. CONCLUSIONS AND FUTURE PERSPECTIVES.....	27
6. REFERENCES.....	29
ATTACHMENTS.....	32

## *Index of figures*

Figure 1.....	2
Figure 2.....	3
Figure 3.....	4
Figure 4.....	6
Figure 5.....	14
Figure 6.....	19
Figure 7.....	20
Figure 8.....	21
Figure 9.....	22
Figure 10.....	23
Figure 11.....	24
Figure 12.....	26

## *Index of tables*

Table 1.....	9
Table 2.....	12
Table 3.....	17
Table 4.....	18
Table 5.....	22
Table 6.....	25
Table 7.....	27

## *Abbreviations*

Abs: Absorbance  
ABTS: 2,2'-azino-bis(3-ethylbenzothiazoline-6-sulphonic acid)  
AD: Alzheimer's disease  
ANOVA: Analysis of variance  
APC: Antigen presenting cell  
ATP: Adenosine tri-phosphate  
 $A\beta$ : Beta-amyloid  
BBB: Brain Blood Barrier  
CD-(number): Cluster of differentiation, (number)  
CDRE: Calcineurin-Dependent Response Element  
CN: Calcineurin  
CNB1: Calcineurin regulatory B subunit  
CNS: Central Nervous System  
COX-2: Cyclo-oxygenase-2  
CR3: Complement receptor type-3  
CSM: Complete supplement mixture  
DHE: Dihydroethidium  
DMEM: Dulbecco's modified Eagle's medium  
DMSO: Dimethyl sulfoxide  
DNA: Deoxyribonucleic acid  
DNAse: Deoxyribonuclease  
ECL: Enhanced chemiluminescence  
ELISA: Enzyme linked immuno sorbent assay  
FACS: Fluorescence-activated cell sorting  
FBS: Fetal Bovine Serum  
Fc $\gamma$ R: Fragment crystallizable-gamma receptor  
FDW: Fruit dry weight  
FIC: Fluorescence intensity counts  
FITC: Fluorescein isothiocyanate  
FSC: Forward scatter  
GAE: Gallic Acid Equivalent  
HRP: Horseradish Peroxidase  
Iba-1: Ionized calcium binding adapter molecule-1  
IKK: I $\kappa$ B kinase  
IL(number): Interleukin, (number)  
iNOS: inducible Nitric oxide synthase  
I $\kappa$ B: Inhibitor of nuclear factor kappa B  
JHI: James Hutton Institute  
LOX: Lipoxygenase

LPS: Lipopolysaccharide  
MAC1: Macrophage antigen complex 1  
MAP: Mitogen-Activated Protein  
MAPK: Mitogen-Activated Protein Kinase  
MBA: Membrane blocking agent  
MCP-1: Monocyte chemoattractant protein-1  
MFI: Median fluorescence intensity  
MHC (I and II): Major Histocompatibility Complex (class 1 or class 2)  
MS: Mass spectrometry  
NADPH: Nicotinamide adenine dinucleotide phosphate  
NEAA: non-essential amino acids  
NFAT: Nuclear factor of activated T-cells  
NF- $\kappa$ B: Nuclear factor kappa B  
NLS: Nuclear localization signals  
NO: Nitric oxide  
NOS: Nitric oxide synthases  
ONPG: Ortho-Nitrophenyl- $\beta$ -galactoside  
PAMP: Pathogen-associated molecular pattern  
PBS: Phosphate Buffer Saline  
PD: Parkinson's disease  
PGE2: Prostaglandin E2  
PHOX: Phagocyte NADPH oxidase  
PRR: Pattern recognition receptor  
qPCR: Quantitative/real-time Polymerase Chain Reaction  
RIPA: Radioimmunoprecipitation assay  
ROS: Reactive Oxygen Species  
SCM: Synthetic Complete Medium  
SD: Standard Deviation  
SDS: Sodium dodecyl sulfate  
SDS-PAGE: Sodium dodecyl sulfate - Polyacrylamide gel electrophoresis  
SE: Standard Error  
SSC: Side scatter  
TBS: Tris-buffered saline  
TBST: Tris-buffered saline with Tween20  
TLR: Toll-like receptors  
TNFR: Tumor necrosis factor receptor  
TNF- $\alpha$ : Tumor necrosis factor - alpha  
YNB: Yeast nitrogen base  
 $\alpha$ -SIN: Alpha-synuclein



## ***Abstract***

Microglia are the resident innate immune cells in the central nervous system (CNS), representing the first defense line of the neural parenchyma. However, its chronic activation is implicated in neurodegenerative disorders by the uncontrolled release of diverse molecular mediators such as inflammatory cytokines.

Among all dietary phytochemicals, polyphenols are the major anti-inflammatory molecules provided by some plants. As example, raspberries are an enriched natural source of polyphenols such as ellagic acid, flavanols; and phenolic acids. However, digestion strongly modifies the structure of polyphenols, producing metabolites with different bioactivities. Thus, it is imperative the study of digested polyphenols for a better elucidation about their effects.

The main goal of this study was to evaluate the bioactivity of raspberry polyphenols as neuroinflammatory attenuators. The fractions studied were composed by polyphenols that are bioaccessible to blood serum, obtained from *in vitro* digestion of five different quasi-isogenic raspberries. Furthermore, N9 murine microglial cell line was implemented as model of neuroinflammation and the range of non-cytotoxic concentrations of each fraction was determined. Then, the neuroinflammatory attenuation induced by each digested fraction in LPS-stimulated microglia was evaluated and compared. As result, some of the fractions attenuated microglial pro-inflammatory activation, significantly decreasing the expression of membrane protein CD-40 (marker of microglial activation) and the production of the pro-inflammatory markers, nitric oxide (NO), tumor necrosis factor- $\alpha$  (TNF- $\alpha$ ) and intracellular superoxide ( $O_2^{\cdot-}$ ).

Additionally, a yeast model of inflammation was used as a mechanistic tool to elucidate the molecular mechanisms underlying the anti-inflammatory activity of the digested raspberry fractions. The results showed that these compounds inhibit the yeast Crz1/calcineurin pathway, which is homologous to the mammalian nuclear factor of activated T-cells (NFAT)/calcineurin, suggesting that they may prevent microglial neuroinflammation through this pathway.

## ***Keywords***

Polyphenols, raspberries, digested fractions, neuroinflammatory attenuation

## Resumo

Quando exposto a diversas agressões tais como infeções, toxinas ou traumatismos, o sistema nervoso central medeia uma resposta inflamatória complexa e ao mesmo tempo dinâmica. Esta resposta inclui uma curta e eficiente ativação do sistema imunitário, que geralmente é mediada pela população de células imunitárias residentes – a microglia.

A microglia representa cerca de 12% do tecido cerebral e participa na primeira linha de defesa do parênquima neural. Num estado não ativado apresenta uma morfologia ramificada, tendo como função a continua monitorização do espaço que rodeia os neurónios. Uma vez exposta a um estímulo pro-inflamatório, a microglia entra num estado ativado que, tipicamente, é acompanhado de uma transição da morfologia para uma forma ameboide, o que favorece a fagocitose. Neste estado, a expressão de muitos recetores de superfície relacionados com a resposta imunitária é aumentada. São também induzidas muitas vias de sinalização celular que conduzem à secreção de diferentes compostos pro-inflamatórios. Por exemplo, compostos como o fator de necrose tumoral –  $\alpha$  (TNF- $\alpha$ ), a interleucina -  $1\beta$  (IL- $1\beta$ ), ou as espécies reativas de oxigénio, são regulados por diferentes vias de sinalização celular tais como a via do fator nuclear –  $\kappa B$  (NF- $\kappa B$ ), a via do fator nuclear das células T ativadas (NFAT) ou a vias das cinases MAP (MAPK).

Muitos dos agentes pró-inflamatórios conhecidos e descritos são pesticidas como o paraquato, dieldrina, lindano ou rotenona; outros são toxinas como os lipopolissacarídeos (LPS) provenientes da membrana exterior de bactérias gram-negativas. Geralmente, estes agentes estão associados a casos patológicos, nos quais a microglia adquire um estado de sobreativação crónica. Nestes casos, muitos compostos mediadores da inflamação são continuamente e abundantemente secretados pela microglia, causando lesões e provocando ativação das vias de apoptose nas células neuronais vizinhas. Elevados e contínuos níveis de produção de óxido nítrico, de espécies reativas de oxigénio e de citocinas estão descritos como patológicos em várias doenças neurodegenerativas, tais como *Alzheimer*, *Parkinson*, *Huntington*, Esclerose Múltipla ou Esclerose lateral amiotrófica. Por sua vez, proteínas como a  $\alpha$ -sinucleína ou a  $\beta$ -amilóide, que estão descritas nas doenças de Parkinson e Alzheimer, respetivamente, atuam como agentes pro-inflamatórios, perpetuando e intensificando a resposta inflamatória. Nos casos mais severos, ocorre uma fragilização da barreira hematoencefálica, o que permite a entrada de macrófagos periféricos para a progressão e intensificação do processo inflamatório.

Os hábitos alimentares atuais também promovem uma ação pró-inflamatória que contribui para a progressão de algumas das doenças crónicas anteriormente citadas. A dieta

atual envolve o elevado consumo de carnes vermelhas, doces, alimentos ricos em gorduras e bebidas gaseificadas, enquanto há um baixo consumo de fruta fresca, nozes, vegetais, cereais e fontes naturais de ómega-3 como o peixe.

Muitos estudos com vista à atenuação da neuroinflamação comprovaram que a dieta, e em especial, o consumo de algumas classes de polifenóis provenientes da fruta e dos vegetais, parece ter um efeito positivo nesse contexto. No entanto, é importante mimetizar os diversos processos de transformação que ocorrem nos polifenóis durante a digestão *in vivo*, uma vez que essas transformações alteram drasticamente a sua função biológica. Uma das formas de mimetizar a digestão é o recurso à utilização de modelos de digestão *in vitro*, a partir dos quais se obtêm as frações digeridas dos polifenóis. Os metabolitos constituintes destas frações são semelhantes àqueles que estariam bioacessíveis às células alvo *in vivo*.

A procura de polifenóis cujos efeitos sejam benéficos face às mais diversas patologias, como o cancro ou as doenças neurodegenerativas, levou ao aumento do estudo dos pequenos frutos. Estes frutos possuem uma vasta gama e um elevado teor em polifenóis, o que propicia a sua utilização na investigação científica. Em particular, as espécies do género *Rubus* têm sido referenciadas como altamente benéficas para a saúde.

No presente estudo, avaliou-se a eventual atenuação da neuroinflamação promovida por cinco frações digeridas de diferentes framboesas em células de microglia. As cinco cultivares de framboesa utilizadas provêm de um banco de germoplasma do *James Hutton Institute*, caracterizando-se por diferirem entre si na constituição nas diferentes classes de polifenóis. Para a obtenção das frações digeridas, as diferentes framboesas quasi-isogénicas foram liofilizadas, solubilizadas em água e submetidas a um modelo de digestão *in vitro*. De cada tipo de framboesa resultaram duas frações distintas, uma fração digerida bioacessível ao cólon e uma fração digerida bioacessível ao soro do sangue. Para o presente trabalho apenas foram utilizadas as frações bioacessíveis ao soro do sangue. Todo o processo da digestão *in vitro* até à obtenção das frações foi desenvolvido pelo Dr. Derek Stewart, do *James Hutton Institute*.

A primeira tarefa deste trabalho foi a implementação do modelo de neuroinflamação com a linha celular N9 de microglia de ratinho. Para tal, as células foram estabelecidas em cultura *in vitro* e estimuladas com *LPS*. Devido à complexidade inerente à resposta inflamatória mediada pela microglia, foi necessário identificar e aceder a diferentes marcadores pró-inflamatórios típicos da microglia ativada, através de diferentes técnicas. Para a determinação do óxido nítrico libertado pelas células, foi quantificado o teor em nitritos no meio de cultura através da reação de Griess. O fator de necrose tumoral –  $\alpha$  (*TNF- $\alpha$* ) foi quantificado no meio de cultura, recorrendo à técnica de *Enzyme Linked Immuno Sorbent Assay (ELISA)* quantitativa. O radical superóxido e a proteína de membrana CD-40 foram ambos quantificados recorrendo à técnica de citometria de fluxo.

A tarefa seguinte foi a avaliação da citotoxicidade das frações de framboesa digerida, como forma de determinar, dentro da gama de concentrações descritas como fisiológicas, quais as concentrações não tóxicas adequadas para a sua utilização na linha celular N9 de microglia de rato.

A última tarefa foi a avaliação da atenuação da neuroinflamação promovida pelas frações digeridas na linha celular N9 de microglia de rato. Para tal, as células foram pré-incubadas com as diferentes frações digeridas de framboesa e seguidamente estimuladas com LPS. De seguida, foram quantificados os diferentes marcadores previamente validados na primeira tarefa (óxido nítrico, TNF- $\alpha$ , CD-40 e radical superóxido). Como resultado, três das frações digeridas revelaram grande consistência na significativa redução da produção e expressão dos diversos marcadores na linha de microglia N9, o que evidencia o seu forte contributo para a atenuação da neuroinflamação. Por outro lado, as restantes duas frações não exibiram um efeito anti-inflamatório consistente para todos os marcadores inflamatórios, sendo que em alguns desses marcadores não se observaram reduções significativas na produção/expressão relativamente aos controlos positivos da inflamação.

Adicionalmente, como ferramenta mecânica foi utilizado um modelo de inflamação construído em levedura. A utilização deste modelo revelou que, de alguma forma, os metabolitos presentes nas frações de framboesa digerida interferem na regulação da via celular calcineurina / Crz1, reprimindo a sua indução pela dicitão cálcio ( $Ca^{2+}$ ). Esta via de sinalização é regulada de uma forma semelhante nos mamíferos, sendo que *CRZ1* é ortólogo de *NFAT*, que, por sua vez, está intrinsecamente relacionado com a inflamação. Assim, os resultados obtidos com o modelo de inflamação em levedura sugerem que uma das vias pela qual os metabolitos presentes nas frações digeridas de framboesa atenuam a neuroinflamação na microglia é pela via da calcineurina - *NFAT*.

Por último, os resultados da atenuação da inflamação na microglia e nos ensaios em levedura foram comparados com as diferentes composições químicas em polifenóis de cada uma das frações digeridas utilizadas. Por conseguinte, algumas classes de polifenóis, tais como os conjugados de ácido elágico, foram identificadas como relacionadas com o poder anti-inflamatório das frações.

### ***Palavras-chave***

Polifenóis, framboesa, quasi-isogénicas, digestão *in vitro*, atenuação da neuroinflamação

## *1. Objectives*

Neuroinflammation can be initiated in response to a variety of injuries, including infection, traumatic brain injury or toxic metabolites<sup>1</sup>. In the central nervous system, including the brain and spinal cord, microglia are the resident innate immune cells that mediate the inflammatory response to these injuries<sup>1</sup>.

In the present study, the main objective was the evaluation of the neuroinflammatory attenuation that comes from the treatment with five different digested quasi-isogenic raspberry fractions. These fractions were obtained from the in vitro digestion of germplasm raspberry lines, in James Hutton Institute.

The first task was the implementation of N9 murine microglial cell line as a model of neuroinflammation, by accessing diverse pro-inflammatory and activation markers typical of LPS-stimulated microglia. Different techniques such as ELISA, griess reaction, flow cytometry and western blot were used for that purpose. Secondly, the cytotoxicity of the digested raspberry polyphenolic fractions was assayed in order to guarantee the range of non-toxic concentrations while using also physiological concentrations.

As the final task, the inflammatory attenuation from the treatment with each fraction in LPS-stimulated microglia was evaluated by the analysis of the markers previously validated in the model implementation. Also, a yeast model of inflammation was used as mechanistic tool for the evaluation of the anti-inflammatory bioactivity of the digested raspberry fractions as inhibitors of Crz1/calcineurin pathway.

## 2. Theoretical fundamentals

### 2.1. Microglia: the innate immune cell of central nervous system

Microglia are the resident innate immune cells in the central nervous system (CNS) and comprise approximately 12% of the brain tissue<sup>2</sup>. They are involved in the first defense line for the neural parenchyma, releasing diverse molecular mediators such as inflammatory cytokines.

Generally, it is accepted that the original microglia population differentiates from cells of the myeloid lineage, which occurs in early embryonic development. This could justify the common expression of the majority of surface markers of monocytes and macrophages: CD1a, CD2, CD4, CD16, CD18, CD40, CD45, major histocompatibility complex (MHC) class I and II, among many others<sup>3</sup>.

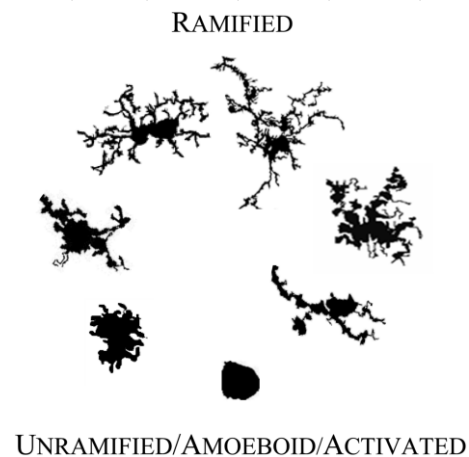


**Figure 1** – Microglia are morphologically and functionally dynamic cells. They are able to change from highly ramified shapes (non-activated cells) to completely lacking processes cellular bodies (activated cells)<sup>4</sup>.

In addition, cell surface receptor-ligands, such as, CD-200 are present, contributing to maintenance of neuron-microglia communication in the CNS<sup>9</sup>.

Once exposed to pro-inflammatory triggers such as pathogens, brain injuries, dead or dying cells and immunological stimuli, microglia cells respond by modifying its ramified morphology to the amoeboid shape, favoring phagocytic activity<sup>10</sup>. These alterations are also followed by changes in signaling cascades, which promote upregulation in the expression of many cell surface receptors, as well an increase in the production of other pro-inflammatory mediators<sup>11, 12</sup>. As example, the release of tumor necrosis factor-alpha (TNF- $\alpha$ ) is also a reliable marker of microglial activation<sup>13, 14</sup>.

Although, during the development of some neurodegenerative disorders, microglia is reported to acquire a prejudicial overactivated stage that persists chronically. At this stage, the continuous high release of many of the pro-inflammatory mediators such as cytokines<sup>15, 16</sup>,

reactive oxygen species (ROS)<sup>17</sup> or nitric oxide (NO)<sup>18</sup> are described as implicated in the pathology of Alzheimer's disease (AD), Parkinson's disease (PD), Huntington's disease, Multiple sclerosis, Amyotrophic lateral sclerosis and other neurodegenerative disorders. In addition, those mediators can also strongly contribute for cerebrovascular damage in diverse neurodegenerative disorders such as AD and PD<sup>19</sup>.

## 2.2. Neuroinflammation

The CNS mediates a dynamic immune and inflammatory response when exposed to infections, trauma, stroke, toxins and other stimuli capable of inducing an activation of the innate immune system. This response is usually mediated by microglial activation. Notwithstanding, microglial activation can have either positive or detrimental effects on neurons, according to the duration and amounts of cytokines and growth factors secreted<sup>20</sup>.

Within activation, microglia produce inflammatory mediators that are essential to protect the CNS against injuries. Also, damaged or dead cells increase the phagocytic activity of activated microglia<sup>21</sup>. However, it is typically a short-lived activation with no harmful effects for other neuronal cells. It is believed that this acute microglial activation is beneficial for CNS, contributing for host protection and tissue repair<sup>22</sup>.

On the other hand, chronic neuroinflammation persists long time after the initial injury or trigger and it is often a self-perpetuating event. Many pro-inflammatory mediators such as cytokines are highly increased and sustained<sup>15</sup>. Also, it occurs a notable augmentation of oxidative and nitrosative stress that persists chronically, injuring surrounding neuronal cells and promoting diverse neurodegenerative disorders<sup>23</sup>.

With chronic and sustained states of neuroinflammation, there is commonly a compromise of the blood brain barrier (BBB) which increases infiltration of peripheral macrophages into the brain neural parenchyma to further perpetuate the inflammation<sup>24</sup> (Figure 2).

Whether neuroinflammation is beneficial or harmful to the brain, critically depends on the duration and intensity of the inflammatory response<sup>25, 26</sup>.

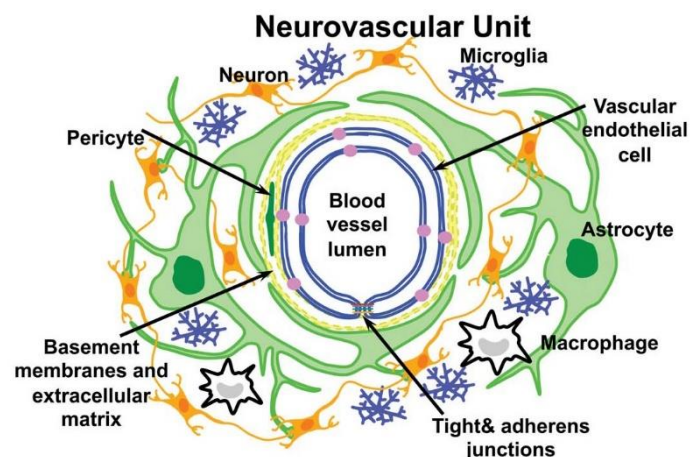


**Figure 2** – Schematic representation of the neurovascular unit that constitutes the Blood-brain barrier (BBB). Vascular endothelial cells form the blood vessel and associate with astrocyte and pericytes forming the basal lamina. Other components of the neurovascular unit are neurons and microglia. Macrophages can also infiltrate during severe neuroinflammatory events. Figure adapted from C. L. Willis, *Toxicol Pathol* 39, 172 (2011).

### 2.2.1 – Markers of microglial activation

Because microglial activation is a complex and dynamic process, it is not simple to identify and conjugate the different molecular players. However, several pathways<sup>27-29</sup> are implicated and some resultant molecules are described as reliable activation markers.

- **Nuclear factor kappa B (NF-κB) pathway**

Nuclear factor kappa B (NF-κB) is a transcription factor that regulates the expression of inducers and effectors at many points in the complex networks related to the response to pathogens<sup>30, 31</sup>. However, this protein extends its transcriptional regulation of the immune response, by influencing also gene expression pathways that impact cell survival, differentiation and proliferation. Because of these wide spectrum implications, the dysregulation of NF-κB is normally described in various pathological situations, including neuroinflammatory disorders<sup>32-34</sup>.

The NF-κB dimers are present in the cytoplasm in an inactive state, sequestered by inhibitory IκB proteins, which mask the nuclear localization signals (NLS). The activation process of this transcriptional factor is mediated by the IκB kinase (IKK) complex. When activated by pro-inflammatory stimulus, such as lipopolysaccharide (LPS)<sup>35</sup>, ROS<sup>36</sup>, TNFα<sup>37</sup> or interleukin 1-beta (IL-1β)<sup>38</sup>, the IKK complex promote phosphorylation and degradation of IκB proteins and subsequent release and activation of NF-κB<sup>39</sup>. Then, NF-κB activation does not require protein synthesis, once the interaction with diverse pro-inflammatory mediators can directly induce the activity of this transcription factor.

- **Nuclear factor of activated T cells (NFAT) pathway**

NFAT is a DNA binding protein required for pro-inflammatory gene expression, which is modulated by calcineurin phosphatase activity<sup>40</sup>.

In its phosphorylated state, NFAT localizes to the cytoplasm, where it remains inactive. Once stimulated, calcineurin dephosphorylates cytosolic NFAT allowing it's translocation to the nucleus where it binds promoters that activate transcription of a large number of genes during an effective immune response<sup>41, 42</sup>(Figure 3). Despite the close involvement of NFAT in the course of pro-inflammatory events, recent findings confirmed also that this transcription factor regulates microglial phenotype, as well as the expression of TNF-α and MCP-1<sup>27</sup> .

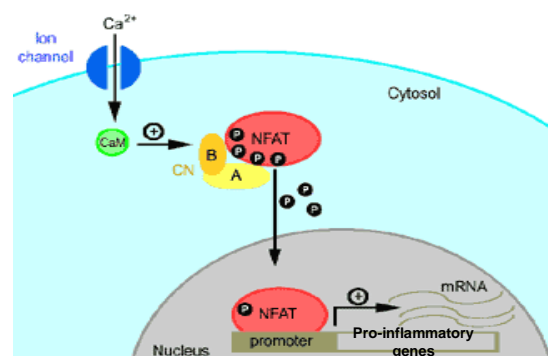


**Figure 3** - The Calcineurin-NFAT signalling pathway. Increase in the intracellular calcium activates the cellular phosphatase Calcineurin (CN) through interaction with Calmodulin (CaM). Activated CN dephosphorylates NFAT, allowing it's translocation for the nucleus were it binds to the promoters of pro-inflammatory genes. Adapted from: ([http://www.angiobodies.com/figuras/uam\\_fig2.gif](http://www.angiobodies.com/figuras/uam_fig2.gif))



- **Mitogen-activated protein kinases (MAPK) pathway**

Mitogen-activated protein kinases (MAPK) constitute a family of serine/threonine/tyrosine-specific protein kinases. These proteins modulate cellular response to diverse external stimuli, such as osmotic stress, heat shock, pro-inflammatory cytokines or LPS. In the CNS, this cellular response is usually mediated by microglia<sup>43, 44</sup>.

Generally, MAPK proteins form a chain of proteins that transduce signals from a cellular surface receptor to the DNA in the nucleus. When the receptor on the cell membrane binds to a signaling molecule, a signal is produced and redirected to the nucleus via MAPKs which communicate by adding phosphate groups to a neighboring protein. The pathway culminates with the signal reaching the nucleus, triggering the expression of proteins that specifically promote alterations in the cell, such as mitosis or inflammatory response.

- **Nicotinamide adenine dinucleotide phosphate-oxidase (NADPH oxidase) pathway**

NADPH oxidase is a membrane-bound enzyme that catalyzes the production of superoxide from oxygen in response to various stimuli, including pathogen-associated molecular patterns (PAMPs), inflammatory peptides<sup>45</sup> and multiple neurotoxins<sup>46</sup>. Superoxide aims to eliminate bacteria and fungi, mainly by interrupting their metabolic activity and promoting lipid peroxidation. This radical can spontaneously produce hydrogen peroxide that is submitted to further reactions, generating additional ROS. This also represents the main mechanism through which microglia produce neurotoxic ROS in response to stimuli<sup>47</sup>.

A recent research suggests that during neuroinflammation, NADPH oxidase plays a critical role in modulating the microglial phenotype towards a pro-inflammatory activated state<sup>48</sup>. In the same study, it was demonstrated that inhibition of NADPH oxidase increases production of anti-inflammatory cytokines such as IL-4, reducing the production of pro-inflammatory cytokines such as TNF- $\alpha$ <sup>48</sup>. Finally, this enzyme is described as an essential player for pro-inflammatory events that occur in some disorders such as AD<sup>49</sup>.

- **Macrophage antigen complex 1 (MAC1)**

This complex, also known as complement receptor type-3 (CR3) or integrin CD-11b/CD-18 is bifunctional, acting as an adhesion molecule, and as a pattern recognition receptor (PRR) which recognizes a diverse set of stimuli, mediating the activation of phagocytes<sup>50, 51</sup>.

The MAC1 receptor is highly expressed in post-mortem brains of patients with AD<sup>8</sup>, matching the microglial activation that occurs in this neurodegenerative disorder. Moreover, MAC1 has been described as a player in NADPH oxidase activation in response to oxidative insults<sup>51-53</sup>. In addition, when MAC1 receptor recognizes a ligand, an induction of the

transcription factor NF- $\kappa$ B signaling pathway and the resulting production of inflammatory factors were verified<sup>54</sup>.

- **A model family of pattern recognition receptors: Toll-like receptors (TLRs)**

TLRs are one of the most studied families of PRRs as they contribute for the immunocompetent cell activation in the CNS and the subsequent pro-inflammatory cascade. In microglia, the expression of TLRs is regulated by signaling cascades during embryonic development and by the exposure to inflammatory triggers, such as pathogens<sup>55</sup>.

There are twelve members of the TLR family identified in mammals that recognize PAMPs from bacteria, fungi, viruses and the host itself<sup>56</sup>. The recognition of PAMPs by these receptors initiates innate immune responses on interaction with infectious agents. In microglia, which expresses the TLRs from 1 to 9<sup>57, 58</sup>, TLR4 is accepted as the primary LPS receptor<sup>59</sup> and has been reported to be a crucial mediator of the inflammatory response to LPS<sup>60, 61</sup>. Additionally, TLR4 also respond to damage associated molecular patterns, released by the injured tissues, and is upregulated upon brain inflammation<sup>61, 62</sup>, strongly suggesting a role of this receptor as pro-inflammatory mediator.

- **Cell surface immune-associated receptors**

Many cell surface receptors associated with the innate immune system response such as MHC molecules are also upregulated during microglial activation through an inflammatory stimulus (Figure 4). The abundance of those molecules during microglial activation allows these cells to act as antigen presenting cells (APC) to T-cells that will then be able to enter the brain in the course of an active infection<sup>6</sup>. As example, CD-40, which is a typical T-Cell surface receptor and a member of the tumor necrosis factor receptor (TNFR) family<sup>63</sup>, is over-expressed by activated microglia<sup>64, 65</sup>. Also, CD-45, the leukocyte common antigen, is highly expressed in constitutively activated microglia from OX2-deficient mice<sup>9</sup>. However, CD-45 level of expression is lower when compared to macrophages<sup>7, 66</sup>, and the same occurs with many other immune-associated receptors.

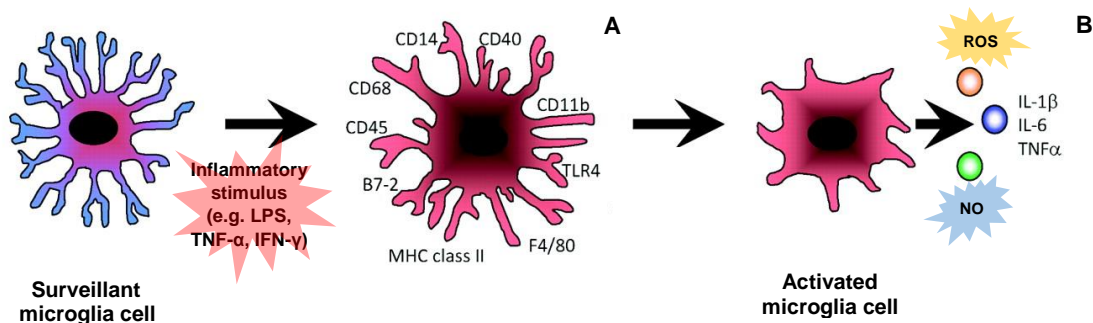


**Figure 4** – Markers of microglial activation. When exposed to an inflammatory stimulus, membrane immune receptors are highly expressed (A) and inflammatory cytokines are secreted, accompanying the shift for the amoeboid morphology (B). Adapted from R. N. Dilger, R. W. Johnson, *J Leukoc Biol* 84, 932 (2008)<sup>67</sup>.

- **Expression of cytokines and chemokines**

Important cytokines and chemokines such as IL-1 $\beta$ , TNF- $\alpha$ <sup>13, 14</sup> (Figure 4) and also monocyte chemoattractant protein-1 (MCP-1) are molecules that constitute good markers of microglial activation. Those molecules are characteristic of macrophage and chemoattractant cells, whereas its abundance in microglia indicates a shift for the phagocytic phenotype<sup>68</sup>.

Chronic releasing of those cytokines by pro-inflammatory microglia may also have a deleterious role, inducing neurodegenerative complications by binding to specific cell surface receptors expressed in neurons and further activating apoptotic pathways<sup>69</sup>. As example, TNF- $\alpha$  binds to tumor necrosis factor receptor-1 which promotes apoptosis in neurons<sup>70</sup>. Dysregulation of this cytokine is implicated in AD<sup>71</sup> and cancer<sup>72</sup>, as well.

- **Production of ROS and NO**

As previously described, NADPH oxidase activation is directly involved in the synthesis of superoxide, which is the main responsible for ROS production in activated microglia. ROS have a crucial role by enhancing host defenses against pathogens; acting also as mediators of cellular signaling for cytokine synthesis<sup>73</sup>; and contributing for the cellular homeostasis. On the other hand, increased ROS production by chronically pro-inflammatory activated microglia can directly damage the surround tissues, contributing for further pro-inflammatory events<sup>74, 75</sup>.

For instance, O<sub>2</sub><sup>•-</sup> is a good example of immediate ROS released by microglia in response to stimulus<sup>76</sup>. Even so, microglial LPS-induced production of O<sub>2</sub><sup>•-</sup> is not mediated through the traditional LPS receptor TLR4; instead, MAC1 is the responsible for NADPH oxidase activation and the subsequent production of O<sub>2</sub><sup>•-</sup><sup>77</sup>.

Also, another important marker excessively released by overactivated microglia during pro-inflammatory events is NO, which have been reported as inducing neuronal death by damaging the mitochondrial electron transport chain, and therefore resulting in neuronal ATP synthesis disruption, increasing the generation of ROS<sup>78, 79</sup>.

- **Other markers: Ion channels**

Another important pro-inflammatory marker that has been suggested as playing an important role in regulation of microglial activation is ionized calcium binding adapter molecule-1 (Iba-1)<sup>80</sup>. It is a calcium-binding protein that is specifically expressed in macrophages and microglia<sup>81</sup>, being upregulated during the activation of these cells. In microglia, Iba-1 expression is up-regulated in response to nerve injury, which occurs in several neurodegenerative disorders<sup>82</sup>.

### **2.2.2 – Common Inflammatory triggers**

An extensive list of pro-inflammatory stimuli, including LPS; pesticides such as paraquat, dieldrin, lindane or rotenone; known disease proteins like beta-amyloid ( $A\beta$ ) or alpha-synuclein ( $\alpha$ -SYN); damaged neurons and even air pollution are capable of inducing pro-inflammatory microglial activation<sup>21</sup>. Some authors have proposed that all these stimuli develop a toxic microglia response due to its misinterpretation as a pathogen<sup>46</sup>.

LPS is one of the most effective stimuli described to promote an inflammatory response. It consists of a cell wall component from gram-negative bacteria and is known by inducing activation of many pathways such as protein kinase C, protein-tyrosine kinases, MAPK, and NF- $\kappa$ B<sup>47</sup>. These pathways are implicated in the release of pro-inflammatory cytotoxic factors, such as NO and some cytokines<sup>83-85</sup>. Its systemic administration in wild-type mice activates microglia and increases expression of pro-inflammatory factors such as TNF- $\alpha$ , MCP-1, IL-1 $\beta$ , and NF- $\kappa$ B<sup>86</sup>.

Another common neuroinflammatory agent is rotenone<sup>87</sup>. It is a lipophilic compound vulgarly used as a natural pesticide (herbicide and insecticide), and it can easily cross the BBB<sup>88</sup>. Due to its high inflammatory efficiency, it is also used to induce Parkinsonism in rodents<sup>89</sup> and has been reported to increase superoxide ( $O_2^{\cdot -}$ ) production by stimulating the microglial phagocyte NADPH oxidase (PHOX)<sup>87</sup>.

### **2.3. Attenuation of neuroinflammation by dietary factors**

As a major aspect of the environment, diet plays a crucial role in the modulation of inflammation. Certain dietary components such as polyphenols, found in fruits, vegetables, nuts, whole grains; and omega-3 fatty acids found in many sea origin foods, seem to promote attenuation of chronic pro-inflammatory processes associated with chronic diseases<sup>90</sup>.

However, since industrial revolution, dietary habits of the Western civilization have changed with the development of agriculture and food processing industry. Nowadays diet is based on high intakes of red meat, sugary desserts, high-fat foods, refined grains, and carbonated beverages, accompanied by a low intake of fresh and dried fruits, nuts, vegetables, whole grains, insoluble fiber, fish, and walnuts. These dietary habits contribute for the increasing of chronic inflammatory diseases verified in the mentioned civilizations<sup>91, 92</sup>. The following table resumes dietary factors that promote or retard inflammation.

**Table 1** - Dietary factors that are described as pro- and anti-inflammatory. Adapted from X. Wu, A. G. Schauss, *J Agric Food Chem* 60, 6703 (2012).

<b>Pro-inflammatory dietary factors</b>	<b>Anti-inflammatory dietary factors</b>
<ul style="list-style-type: none"> <li>• High-fat diet, including hydrogenated unsaturated plant fats ("artificial" trans fats)</li> <li>• Diets with high glycemic index</li> <li>• Diets low in fruits, vegetables, raw nuts, and whole grains</li> <li>• Sugar-sweetened carbonated and non-carbonated beverages</li> <li>• Insufficient intake of fruits, vegetables, nuts, whole grains and omega-3 enriched food</li> <li>• Hidden or delayed food allergies promoting inflammation</li> </ul>	<ul style="list-style-type: none"> <li>• Diets rich in monounsaturated and omega-3 fatty acids</li> <li>• Diets with a greater variety of fruits, vegetables, raw nuts, and whole grains</li> <li>• Diets high in soluble and insoluble fibers</li> <li>• Diets low in refined grains or minimally processed whole grains</li> <li>• Diets rich in polyphenols including tea, cocoa, red wine, berries and fruits.</li> </ul>

### **2.3.1 – Attenuation of neuroinflammation by polyphenols**

Among all dietary phytochemicals, polyphenols are considered the major anti-inflammatory molecules provided by berries, vegetables, tea, coffee, grains and legumes<sup>93</sup>. These important molecules are characterized by one or more aromatic rings with one or more hydroxyl groups, and are derived from plant's secondary metabolism. More than 8000 polyphenols at the whole plant kingdom have been reported, many of them present in food<sup>94</sup>. The molecular structure of most abundant polyphenols found in the human diet is presented in Attachment 1.

The way polyphenols act as anti-inflammatory agents is not straightforward, but it is accepted that they can regulate enzymes involved in the role of inflammatory events. Some of those enzymes are glutathione peroxidase<sup>95</sup>, nitric oxide synthase (iNOS), cyclooxygenase-2 (COX-2), and lipoxygenase (LOX), which are involved in the production of many mediators of inflammation, such as NO, arachidonic acid or prostaglandins<sup>96, 97</sup>.

Recently, the hormesis theory has been associated with some polyphenols as their biological mechanism. Some studies revealed that they can actually promote cellular toxicity and stress at high concentrations<sup>98</sup>. However at the physiologic cellular level, polyphenols are usually found in very low concentrations which promotes a hormetic response, stimulating adaptive cellular stress pathways<sup>98</sup>. Precondition with polyphenols can stimulate those adaptive pathways, becoming more effective in the prevention and attenuation of severe neuroinflammatory processes<sup>99, 100</sup>. As example, LPS-induced NF- $\kappa$ B activation in microglia is inhibited by the pre-treatment with polyphenols<sup>101</sup>.

Increasing evidences suggest that flavonoids inhibit the production of pro-inflammatory cytokines such as TNF- $\alpha$ , IL-6 and IL-1, suggesting its close involvement in pathways such as

NF- $\kappa$ B or MAPK<sup>102, 103</sup>. Catechins, the major polyphenolic components of green tea, are a group of flavonoids with several anti-inflammatory properties. According to clinical trials and animal studies, chronic tea drinking leads to inhibition of low-level inflammation due to alterations in various inflammatory markers<sup>104</sup>. In addition, there is strong evidence that blueberry polyphenols inhibit production of NO, IL-1 $\beta$  and TNF- $\alpha$  in activated microglial cells<sup>105</sup>.

Additionally, many studies show that polyphenols delay and slow the progression of neurodegenerative disorders, such as AD, by inhibiting neuronal apoptosis promoted by release of neurotoxic species and pro-inflammatory mediators<sup>106, 107</sup>.

### **2.3.2 – Polyphenols metabolites**

Despite all the beneficial effects achieved with undigested polyphenols, its utilization is limited because, *in vivo*, those compounds result in metabolites with different biological properties due to digestion, absorption and metabolization.

For example, whereas quercetin exhibits strong anti-inflammatory activity by attenuating NOS production<sup>108</sup> and preventing the release of inflammatory cytokines in microglia<sup>109, 110</sup>, one of its largest metabolites, quercetin-3'-sulfate, failed in evidencing such anti-inflammatory activity<sup>111</sup>.

Conversely, many polyphenol metabolites have stronger anti-inflammatory effects than their precursor molecules. A study comparing 45 different polyphenolic compounds showed that both flavanols (+)-catechin and (-)-epicatechin did not inhibit NADPH oxidase unlike their most common methylated metabolites, which exhibited strong NADPH oxidase inhibition<sup>112</sup>.

Many studies converge at suggesting that polyphenols have positive effects against neurodegenerative disorders, thus these particular molecules are crucial to keep under study. However, the study of polyphenols metabolites is imperative to get conclusions that can be more trustful about its real health benefits.

### **2.3.3 - Raspberry: a fruit with potential anti-neuroinflammatory properties**

Raspberries are edible berries that represent an important commercial crop, widely grown in all temperate regions of the world. These berries belong to genus *Rubus*, from *Rosaceae* family. An important species is the red raspberry (*Rubus idaeus*), which is widely cultivated in Europe and Asia<sup>113</sup>; another is the eastern North American black raspberry (*Rubus occidentalis*)<sup>114</sup>.

Raspberries and other small fruits are known to represent a great source of natural antioxidants<sup>115</sup>, including polyphenols such as ellagic acid, flavanols; and phenolic acids<sup>116</sup>.

Therefore, these fruits have increased their popularity in the human diet. Certainly, one of the most famous antioxidant sub-classes found on these berries are anthocyanins. Although the interest in these compounds first aroused due to its antioxidant properties, most recent studies suggest that the beneficial health effects are also associated with their chemopreventative and anti-inflammatory properties. As example, the beneficial biological activity of black raspberry against esophageal, colon, and oral cancers has been demonstrated<sup>117</sup>. In addition, these fruits are also an enriched natural source of other phytochemicals such as flavonols, phenolic acids, ellagic acids and  $\beta$ -sitosterol, as well as the vitamins C, E and folate.

In respect to anti-inflammatory capacity, anthocyanins<sup>118</sup> and ellagitannins are independently described as biological molecules acting as anti-inflammatory agents. Ellagitannins and their colonic derived metabolites have shown anti-inflammatory capacity in rats, reducing the levels of prostaglandin E2 (PGE2), NO production, iNOS and many other markers<sup>119</sup>. Similarly, another study concluded that ellagitannins and their colonic metabolites also suppressed arthritis incidence and inflammatory markers in the arthritic joints<sup>120</sup>.

Red raspberry polyphenolic-enriched extract, typically a complex mixture, mainly composed by ellagitannins and anthocyanins but also by ellagic acid glycosides and flavonol conjugates<sup>121</sup>, has demonstrated anti-inflammatory properties *in vivo*<sup>118, 122</sup>.






### 3. Materials and methods

#### 3.1. Plant material, *in vitro* digestion and fractions preparation

For this research, 5 different digested raspberry polyphenolic fractions were obtained and provided by Dr. Derek Stewart, from the Division of Enhancing Crop Productivity and Utilisation, at James Hutton Institute, England.

The raspberries were originally harvested from the different germplasm lines (quasi-isogenic cultivars) generated by artificial selection in James Hutton Institute (JHI), Invergowrie, Dundee, Scotland, in 2012 (Table 2). The harvest of each quasi-isogenic raspberry was mixed, then freeze-dried. A chemical characterization of the polyphenolic content present in the fruits was also performed and presented in Attachment 2. The freeze-dried powder was rehydrated by shaking water (2 g in 20 mL) prior to submission to an *in vitro* digestion model, previously described by McDougall et al, 2005<sup>123</sup>. This model mimics gastric digestion under pH 1.7 by in the presence of pepsin incubated with shaking at 0.56 x *g* at 37°C for 2h; and small intestine digestion by the interaction with pancreatin and bile salts. At the end of the digestion process, the resulting digested fractions were dialyzed for 2h at 37°C with a cellulose tube containing NaHCO<sub>3</sub> to neutralize titratable acidity. The solution that entered the dialysis tubing (fraction “IN”) and the solution outside the dialysis tubing (fraction “OUT”) were both collected, representing respectively, the bio-accessible fractions to serum and to colon. Both fractions were applied to a C18 solid phase extraction (SPE) column (GIGA tubes, 1000 mg capacity, Phenomenex Ltd.) for the removal of possible interfering compounds from the *in vitro* digestion model<sup>124</sup>. In the present work, only the “IN” fractions were used (Table 2).

**Table 2** – Different raspberry crops obtained from each of the five quasi-isogenic cultivars. The berries from each cultivar were submitted *in vitro* digestion. The final digested fractions (specifically, the bio-accessible fractions to serum – fractions “IN”) were used at the present work. The correspondent designations attributed during this work are presented below each fruit.

	Glen Enrich	0304F6	00123A7	Tulameen	2J19 “yellow raspberry”
Fruit designation					
Fraction designation	“R1”	“R2”	“R3”	“R4”	“R5”



## **3.2. Microglial model of neuroinflammation**

### **3.2.1 – Cell culture and treatments**

The N9 murine microglial cell line was a gift from Dr. Teresa Faria Pais (Institute of Molecular Medicine, Lisbon). Cells were cultured in EMEM (Eagle Minimum Essential Media) supplemented with 10% fetal bovine serum (FBS) (Gibco®), L-glutamin (200 mM), 1% (v/v) non-essential amino acids (NEAA) (Sigma–Aldrich® - Poole, Dorset, UK) and maintained at 37°C in an humidified atmosphere of 5% (v/v) CO<sub>2</sub>. No antibiotics were used. Cells were detached by agitation before suspension of the culture media with pipette. (No detaching agent, like trypsin, was used). Cell confluence was also monitored, avoiding cells to reach confluences higher than 80%.

For the neuroinflammatory model establishment, N9 murine microglial cells were plated onto 6-well plates ( $5 \times 10^5$  cells . mL<sup>-1</sup>) and cultured overnight to reach a confluence of 50-60%. Then, cells were stimulated with LPS (Sigma–Aldrich® - Poole, Dorset, UK) [100 to 500 ng . mL<sup>-1</sup>] during 24 hours, in order to release pro-inflammatory mediators, such as NO<sup>18</sup> and TNF- $\alpha$ <sup>15</sup> in the media (see 3.2.3 section). CD-40<sup>64</sup> and superoxide<sup>76</sup>, whose expression/production is increased upon microglia activation, were quantified by flow cytometry (see 3.2.3 section). Also, Iba-1<sup>80</sup> was assayed by western blot (see 3.2.3 section).

To test the capacity of the different fractions (see chapter 3.1) in attenuation of neuroinflammation, N9 microglial cells were plated onto 6-well plates ( $5 \times 10^5$  cells . mL<sup>-1</sup>) and cultured overnight to reach a confluence of 40-60%. Then, cells were pre-incubated with the digested raspberry polyphenolic fractions [1 to 1.25  $\mu$ g GAE . mL<sup>-1</sup>] during 2 to 24h. At this stage, FBS concentration was reduced to from 10% to 0.5% (v/v), avoiding protein-polyphenol interactions and further precipitation. It was assured that the reduction of the FBS concentration did not affected the viability and functionality of the cells. After incubation with the fractions, media was discarded and cells were washed once with phosphate buffer saline (PBS) 500  $\mu$ L prior to addition of fresh media with 10% FBS with LPS [100 to 500 ng . mL<sup>-1</sup>]. The inflammatory mediators validated in the model establishment (NO, TNF- $\alpha$ , CD-40 and superoxide) were assessed by using same methodologies.

### **3.2.2 – Protein extraction and quantification**

Protein extraction and quantification was assayed for the normalization of the results and for western blotting. Cell media was removed and 150  $\mu$ L of RIPA buffer [50 mM Tris (CarlRoth® – Schoemperlenstr, Karlsruhe, Germany); 150 mM NaCl (Sigma–Aldrich® - Poole, Dorset, UK); 0.1% (w/v) Sodium dodecyl sulfatate (SDS) (Merck® - Frankfurter Straße, Darmstadt, Germany); 0.05% (w/v) sodium deoxycholate (Sigma–Aldrich® - Poole, Dorset,

UK); 1% (v/v) NP-40; 0.05% (v/v) cocktail protease inhibitors (AppliChem Inc - Mary Avenue, Missouri, USA) ; and 0.4% (v/v) DNase (Roche® – Basel, Switzerland)] were added. After incubation for 15 minutes at room temperature, the lysate was scrapped, transferred into microtubes and centrifuged (10 minutes; 4°C; 8000 x g). The lysate was stored at -80°C and protein determination was performed by Lowry protein assay<sup>125</sup>.

### 3.2.3 – Determination of pro-inflammatory and activation markers

- **Nitric Oxide measurement by Griess Reaction**

Because of the relatively short half-life of NO in aqueous solution, its quantitative measurement usually is indirectly accessed by the quantification of its oxidized products, nitrite and nitrate, which are regarded as suitable markers of NO release. The choice of the detection method depends on the type of cell and on the released quantity<sup>126, 127</sup>.

For this experiment, it was used the Griess Reagent (Sigma–Aldrich® - Poole, Dorset, UK), which measures nitrite (Figure 5). For analysis, 100 µL of cell culture medium were quickly removed from each well of the culture plate and added to a 96-well plate for reading. For nitrite quantification, a standard curve of sodium nitrite [0 to 25 µM] was prepared. Equal volumes of Griess reagent were added to each well. The plate was incubated for 15 minutes at room temperature and the absorbance (Abs) was read at 540 nm.

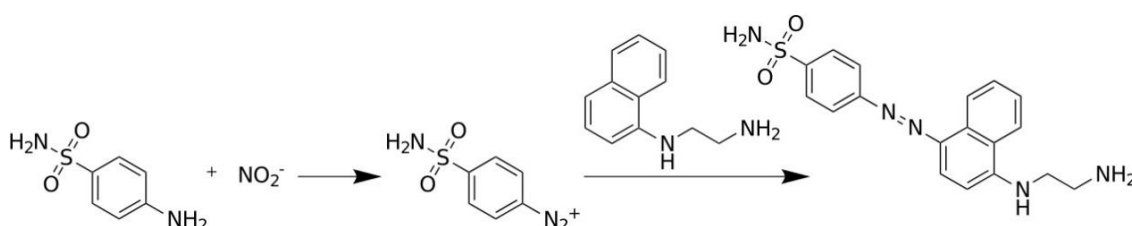


**Figure 5** - Griess reaction scheme. This reaction allows the detection of organic nitrite compounds and was first described in 1858 by Peter Griess. This image belongs to the public domain, and contains no original authorship.

- **TNF-α quantification by ELISA**

Cell supernatants were harvested after 24h and stored at -80°C until analysis. TNF-α release was assayed by sandwich ELISA (Enzyme-Linked Immunosorbent Assay) according to the manufacturer's instructions (PeproTech®; Princeton Business Park, Rocky Hill NJ, United States)<sup>128</sup>. All the reagents and plates used were provided in the kit. For the standard, recombinant murine TNF-α was diluted from 2 ng . mL<sup>-1</sup> to zero in diluent. Antigen-affinity purified goat anti-murineTNF-α diluted 1 µg . mL<sup>-1</sup> in PBS was used as capture antibody. As detection antibody, it was used a biotinylated antigen-affinity purified goat anti-murineTNF-α diluted 0.25 µg . mL<sup>-1</sup> in diluent. As substrate, Avidin-HRP conjugate diluted 1:2000 (v/v) in diluent was used.

Finally, as liquid substrate, 2,2'-azino-bis(3-ethylbenzothiazoline-6-sulphonic acid) (ABTS) was used in the stock concentration. The plate was incubated at room temperature in a Synergy HT microplate reader, from Biotek<sup>®</sup> for 35 minutes, with 5-minute intervals Abs<sub>405</sub> readings.

- **CD-40 and superoxide (O<sub>2</sub><sup>-</sup>) quantification by flow cytometry**

Culture media was discarded and 1 mL PBS was added to detach N9 adherent cells, which were then incubated with 1 mL mouse anti-FcγR (same as CD-16/32, from E-Biosciences) in FACS buffer (PBS containing 2% fetal calf serum and 0.01% NaN<sub>3</sub>) for 30 minutes at 4°C before staining. Anti-FcγR was required for the blocking of Fc-mediated reactions with other specific antibodies<sup>129</sup>. Cells were spun down at 1000 x g, washed once with 500 μL FACS buffer and doubly stained with 5 μg . mL<sup>-1</sup> mouse anti-CD40 conjugated with fluorochrome FITC (clone 3/23, from BD Biosciences<sup>®</sup>); and with 5 μg . mL<sup>-1</sup> DHE probe (Dihydroethidium, Invitrogen<sup>™</sup>, Carlsbad, CA, USA) as superoxide indicator. Events were acquired using CUBE 6 cytometer, from Partec<sup>®</sup>. Post-acquisition analysis was done with the software FSC express 4 flow research edition<sup>®</sup>.

- **Iba-1 determination by Western Blot**

For Western Blot analysis, 40 μg of total protein lysate from each treatment were separated by SDS-PAGE on a 12% (w/v) acrylamide gel. After electrophoresis, proteins were transferred to a polyvinylidene difluoride membrane, during 90 minutes at 70 Volt (V), 4°C. The membrane was blocked in a solution of 5% (w/v) of membrane blocking agent (MBA) (GE Healthcare<sup>™</sup>, Wilmington, MA, USA) diluted in TBST (50 mM Tris; 150 mM NaCl; 0.05% Tween 20), and incubated for 1h with agitation at room temperature. Then, the membrane was incubated primary antibody [rabbit anti-iba1 (0.7 μg . mL<sup>-1</sup>) from WAKO] overnight, at 4°C. After washing 3x with TBST for 5 minutes, secondary antibody was added [goat anti-rabbit IgG HRP-conjugated (1:300), from Millipore] and the membrane incubated for 2h, with agitation at room temperature. Membrane was washed 3x during 5 minutes with TBST and additionally washed 1 minute with TBS (50 mM Tris; 150 mM NaCl) prior to enhanced chemiluminescence substrate (ECL) addition (PheMtoMax Super Sensitive Chemiluminescence HRP Substrate, Rockland, Gilbertsville, USA). Proteins were visualized by chemiluminescent detection using Molecular Imager ChemiDoc XRS (Quantity One<sup>™</sup> software v.4.6.6; BioRad<sup>®</sup>, Amadora, Portugal).

### **3.2.4 – Cytotoxicity assays**

Cytotoxicity of raspberry digested polyphenolic fractions was tested with cell viability assay (CellTiter-Blue Cell Viability Assay, Promega®). This assay uses the indicator dye resazurin to measure the metabolic capacity of cells as an indicator of cell viability. Viable cells retain the ability to reduce resazurin into resorufin, which is highly fluorescent. Nonviable cells rapidly lose metabolic capacity, do not reduce the indicator dye, and thus do not generate a fluorescent signal<sup>130</sup>.

Cells were plated into 96-well plates ( $5 \times 10^5$  cells  $\cdot$  mL<sup>-1</sup> for final volumes of 100  $\mu$ L per well). After 24 hours of growth, four concentrations (0.25; 0.5; 1 and 2  $\mu$ g GAE  $\cdot$  mL<sup>-1</sup>) of the five digested raspberry fractions were applied. The fractions were dissolved in culture media with 0.5% FBS to avoid major protein-polyphenol interactions and further precipitation. After 21h of incubation with fractions, 20 $\mu$ L of CellTiter-Blue reagent was added to each well. The plate was briefly shaken and incubated again with standard cell culture conditions for 3 hours (performing 24h of total incubation time with fractions). Fluorescence values were recorded in a Synergy HT microplate reader, from Biotek® and normalized for viability percentage relatively to control.

## **3.3. Yeast model of inflammation**

### **3.3.1. Characterization of *Saccharomyces cerevisiae* model of inflammation**

As previously described in the Theoretical Fundamentals section, NFAT modulates microglial activation. This transcription factor has an orthologous gene in yeast – CRZ1. Crz1 is also regulated by calcineurin, a calcium dependent enzyme, in a very similar manner as NFAT does in mammalian cells<sup>131</sup>. When dephosphorylated by calcineurin, Crz1 translocates from the cytosol to the nucleus and binds to the calcineurin-dependent response element (CDRE)<sup>132, 133</sup>. While in mammals NFAT binds to diverse promoters that activate pro-inflammatory gene expression<sup>40, 41</sup>, in yeast, Crz1 binding to CDRE promotes activation of genes related to the response against cellular stress, such as ion pumps<sup>134, 135</sup>. These regulatory similarities are the basis for the use of this microorganism as an eukaryote model of inflammation.

YAA5, a *S. cerevisiae* transgenic strain obtained from the wild-type BY4742, makes use of  $\beta$ -galactosidase expression as a reporter system to infer the anti-inflammatory potential of compounds. Additionally, the strains YAA6 and YAA7 are both used as negative controls. While YAA6 carry a deletion of CRZ1, YAA7 is devoid of CNB1, which encodes the regulatory subunit of calcineurin. The genotypes of each strain are presented in the Table 3<sup>136</sup>.

**Table 3** - *S. cerevisiae* strains used in this work. (From, R. T. Ferreira et al., *Microbiology* 158, 2293 (2012)).

Strain	Genotype	Source or reference
BY4742	MATa his3 leu2 lys2 ura3	EUROSCARF*
YAA5	MATa his3 leu2 lys2 ura3 aur1 : : AUR1-C-4xCDRE-lacZ	Araki et al. (2009)
YAA6	MATa his3 leu2 lys2 ura3 YNL027W : : HIS3MX4 aur1 : : AUR1-C-4xCDRE-lacZ	Araki et al. (2009)
YAA7	MATa his3 leu2 lys2 ura3 YKL190W : : kanMX4 aur1 : : AUR1-C-4xCDRE-lacZ	Araki et al. (2009)

\* EUROpean Saccharomyces Cerevisiae ARchive for Functional analysis.

Calcium is the most common used inducer of Ca<sup>2+</sup>-signaling pathways<sup>137</sup>, since it is captured and accumulated by calmodulin, which can effectively stimulate calcineurin phosphatase activity<sup>138</sup>. However, other molecules/ions are described as indirect inducers of the system<sup>139</sup>, such as Mn<sup>2+</sup> or Li<sup>+</sup>.

### 3.3.2 – $\beta$ -galactosidase assays

Quantification of  $\beta$ -galactosidase activity was performed using different colorimetric substrates. Qualitative measurements were carried out in agar plates where yeast colonies were overlaid with an agarose solution containing 5-bromo-4-chloro-3-indolyl- $\beta$ -D-galactopyranoside (X-gal) (ImmunoSource® - Ruiterslaan 29, Zoersel, Belgium). Quantitative measurements were performed in a 96-well plate with cell lysates exposed to the colorimetric substrate Ortho-Nitrophenyl- $\beta$ -galactoside (ONPG) (Sigma–Aldrich® - Poole, Dorset, UK).

#### • Qualitative assay

Yeast strains were grown overnight at 30°C with agitation in synthetic complete media (SCM) (Table 4) to the exponential growth phase. In the following day, the Abs<sub>600</sub> was measured and 4 x 10<sup>7</sup> cells were centrifuged at 900 x g for 3 minutes and resuspended in 1 mL SCM. The anti-inflammatory potential of fractions was tested by incubating cells with 100  $\mu$ g GAE . mL<sup>-1</sup> of the five digested raspberry polyphenolic fractions (R1, R2, R3, R4 and R5). Immunosuppressant macrolide drug FK506 (Sigma–Aldrich® - Poole, Dorset, UK) dissolved in dimethylsulfoxide (DMSO) was used as positive control (6  $\mu$ g . mL<sup>-1</sup>). Cells were incubated for 90 minutes at 30°C with agitation. After incubation, cells were centrifuged at 900 x g for 3 minutes and the supernatant was discarded. Cells were washed with three time with PBS to remove polyphenols. The supernatant was completely removed and the cells were resuspended in 5  $\mu$ L of SCM. Cells were spotted onto agar-SCM supplemented or not with 1.8 mM MnCl<sub>2</sub>. Cells were incubated for 90 minutes at 30°C before X-Gal overlay - Agarose solution was applied [0.2% (w/v) SDS; 2 mg . mL<sup>-1</sup> X-Gal (solubilized in dimethylformamide); 0.5% (w/v) agarose; 50% (v/v) Lac Z buffer (8.5 g . L<sup>-1</sup> Na<sub>2</sub>HPO<sub>4</sub>; 5.5 g . L<sup>-1</sup> NaH<sub>2</sub>PO<sub>4</sub> . H<sub>2</sub>O; 0.75 g . L<sup>-1</sup> KCl; 0.246 g . L<sup>-1</sup> MgSO<sub>4</sub> . 7H<sub>2</sub>O)]. After few minutes, cells exhibiting  $\beta$ -galactosidase

activity start to develop the indigo color, which is proportional to the activation of Crz1. Images were recorded each 10 minutes for 2h (Menezes et al; 2003; with modifications).

**Table 4** - Synthetic complete media constitution.

Constituent	Final concentration
Complete supplement mixture (CSM) (QBiogene®)	0.79 g . L <sup>-1</sup>
Yeast nitrogen base (YNB) (Difco®, USA)	0.67% (w/v)
Glucose (Sigma–Aldrich® - Poole, Dorset, UK)	2% (w/v)

- **Quantitative assay**

Yeast strains were pre-cultured in SCM overnight at 30°C with agitation to obtain cells in exponential growth phase. In the following day, cells were diluted in fresh SCM and cultured for 8h at 30°C. Then, Abs<sub>600</sub> was measured and cells were again diluted to obtain cultures with Abs<sub>600</sub> 1 after an overnight incubation. Once reached Abs<sub>600</sub> 1, cells were diluted in fresh SCM to a final Abs<sub>600</sub> 0.1 and 300 µL of cultures were transferred into microtubes. As a pre-treatment, 100 µg . mL<sup>-1</sup> of the five digested raspberry polyphenolic fractions (R1, R2, R3, R4 and R5) were applied. As positive control, 6 µg . mL<sup>-1</sup> of FK506 dissolved in DMSO were used. Final volumes of each pre-treatment were equalized in order to avoid interference in the Abs<sub>600</sub>. Pre-treated cells were incubated for 90 minutes at 30 °C. After incubation, cells were thoroughly resuspended and 150 µL were transferred to a second microtube containing 1.8 mM MnCl<sub>2</sub>. Induced and control cells were incubated for 90 minutes at 30°C. After incubation, microtubes were thoroughly resuspended and 10 µL of the cell suspension from each treatment were transferred onto a 96-well plate containing 20 µL Y-PER cell lysis reagent (Pierce® Protein Research, USA) per well. Three technical replicates were generated from each microtube. The plate was incubated for 20 minute at 30°C for cell lysis. For the β-galactosidase activity quantification, 240 µL of a solution containing 1 mg . mL<sup>-1</sup> ONPG dissolved in Lac-Z buffer (8.5 g . L<sup>-1</sup> Na<sub>2</sub>HPO<sub>4</sub>; 5.5 g . L<sup>-1</sup> NaH<sub>2</sub>PO<sub>4</sub> . H<sub>2</sub>O; 0.75 g . L<sup>-1</sup> KCl; 0.246 g . L<sup>-1</sup> MgSO<sub>4</sub> . 7H<sub>2</sub>O) were added to each well. The plate was incubated in a Synergy HT microplate reader, from Biotek® for 2h at 30°C and absorbance readings at 420 nm were performed every 10 minutes.

### 3.4. Statistics

Data are presented as mean values ± standard errors (SE) or standard deviations (SD). Statistical differences were tested using unpaired one-way ANOVA with Tukey post hoc comparison, and considered significant when p<0.05.

## 4. Results and Discussion

### 4.1. Attenuation of neuroinflammation in murine microglial cell line N9

#### 4.1.1 – Implementation of N9 microglial line as a neuroinflammation model

In order to implement a neuroinflammation model with N9 murine microglial cell line, a set of markers that can easily distinguish activated cells from non-activated cells were monitored after LPS stimulation. Therefore, a battery of compounds that have been described as mediators of microglial activation, such as NO<sup>79</sup>, TNF- $\alpha$ <sup>14</sup>, CD-40<sup>64, 140</sup>, (O<sub>2</sub><sup>-</sup>)<sup>76</sup> and iba-1<sup>82</sup> were evaluated.

N9 microglial cells were stimulated with 100, 300 and 500 ng . mL<sup>-1</sup> LPS for 24 hours and culture media was evaluated for NO and TNF- $\alpha$  levels, by Griess reaction and quantitative ELISA, respectively. Adherent cells were lysated for protein quantification to further normalize the results.

As presented in figure Figure 6, the higher the dose of LPS, the higher is the secretion of NO and TNF- $\alpha$ . Secretion of NO shows a linear dose-response relatively to the tested LPS concentrations ( $y = 0.04x + 14.06$  ;  $R^2 = 0.83$ ), despite not having detected significant difference on the level of NO between treatments. TNF- $\alpha$  quantification seems to describe a different tendency, in which there are significant differences between 100 and 300 ng . mL<sup>-1</sup> LPS, but no significant difference between 300 and 500 ng . mL<sup>-1</sup>.

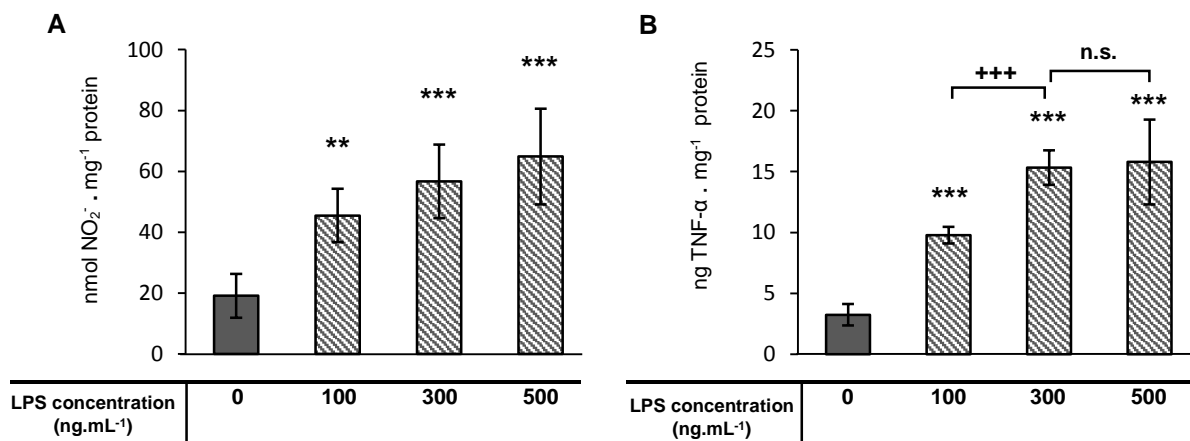


**Figure 6** - Quantification of secreted nitrite measured by Griess reaction (**A**); and secreted TNF- $\alpha$  measured by quantitative ELISA (**B**). Control cells (solid fill bars) and cells stimulated with 100, 300 and 500 ng . mL<sup>-1</sup> of LPS for 24h (striped bars). Statistics are representative of three biological replicates. Data were normalized for the extracted protein in each treatment with  $\pm$  SE. \* represents statistical significant differences between each treatment and the control. \* represents statistical significant differences between indicated treatments. [\*\*\* and \*\*\*  $p < 0.001$ ; \*\*  $p < 0.01$ ; n.s.  $p \geq 0.05$  (not statistically significant)].

To access CD-40 and O<sub>2</sub><sup>-</sup>, N9 cells were stimulated with LPS and stained with specific probes for each marker. Flow cytometry assay was performed as described in the methods. The results show a significant increase in both CD-40 expression and O<sub>2</sub><sup>-</sup> production, with the

increasing LPS dose (Figure 7). Both markers, CD-40 and superoxide increase with LPS stimulation and cell response is clearly detected even for the lower LPS dose.

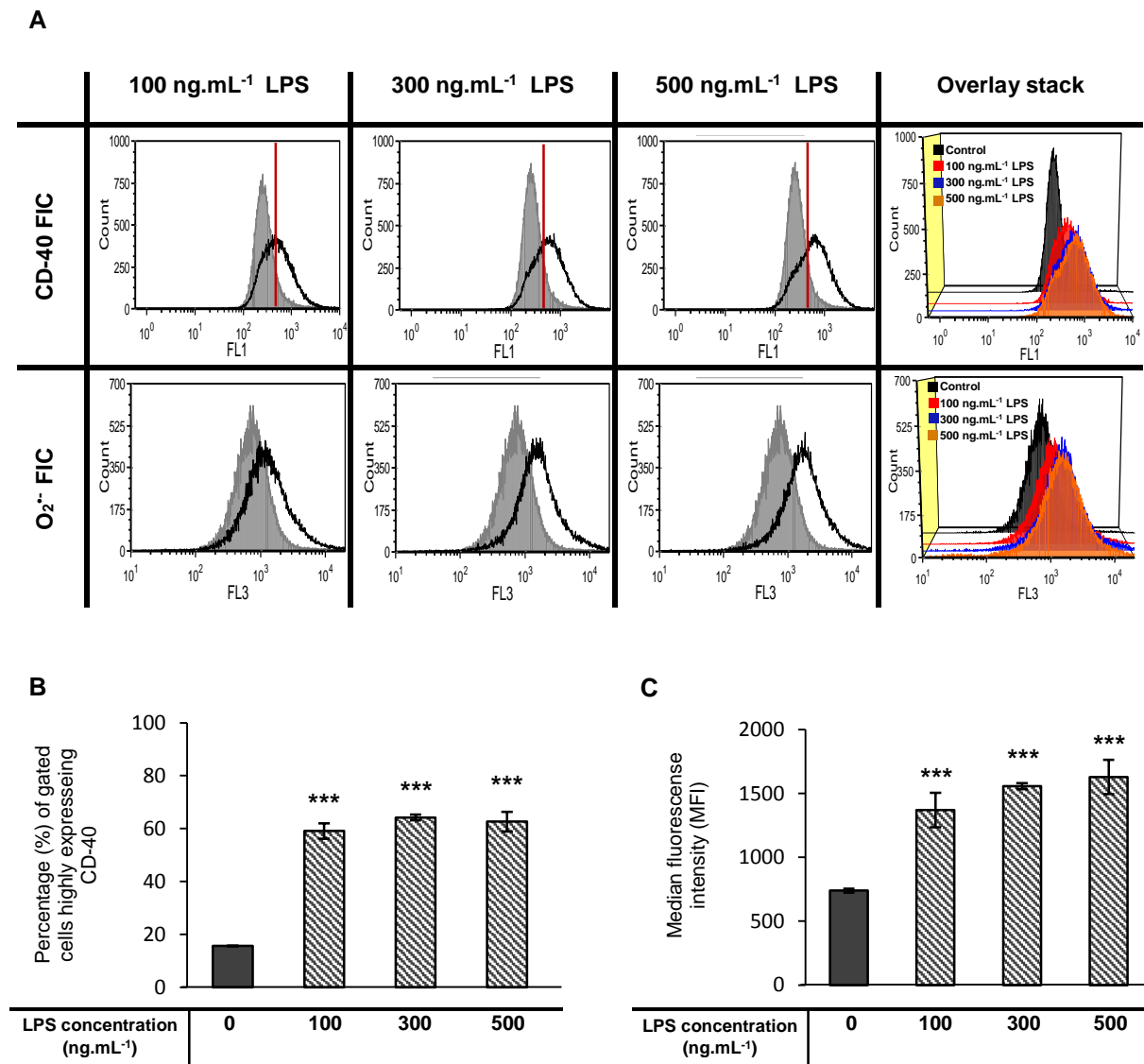


**Figure 7** – Expression of CD-40 and production of intracellular  $O_2^-$  quantified by flow cytometry analysis of N9 microglial cells stimulated with different LPS concentrations [0 (control), 100, 300 and 500 ng . mL<sup>-1</sup> LPS] for 24h. **A** - Histograms of the fluorescence intensity counts (FIC) for CD-40 and  $O_2^-$  in N9 cells after treatment with different LPS concentrations. Each of the first three histograms (for both CD-40 and  $O_2^-$ ) represent the FIC overlays of the cells stimulated with the respective above indicated LPS concentration (**black line**) and the control cells (**solid fill gray**). The red lines on CD-40 histograms indicate the threshold between cells with high and low signal. This threshold was defined relatively to the control, assuming cells as expressing low levels of CD-40 (basal expression). The fourth column for each marker present a 3D overlay stack of the 3 histograms visualized for each LPS concentration, plus the control. **B** - Percentage (%) of gated cells that highly expressed CD-40. **C** - Median fluorescence intensity (MFI) relative to  $O_2^-$  production. Control cells (**solid fill bars**) and cells stimulated with 100, 300 and 500 ng . mL<sup>-1</sup> LPS (**striped bars**). Statistics are representative of three biological replicates for each treatment. Data is presented as mean  $\pm$  SE. \* represents statistical significant differences between each treatment and the control. \*\*\*  $p < 0.001$ .

These results clearly demonstrate that even the lowest LPS concentration tested significantly increased NO, TNF- $\alpha$ , CD-40 and  $O_2^-$  levels, accordingly with the literature<sup>13, 64, 141, 142</sup>. However, from the three LPS concentrations tested, 300 ng . mL<sup>-1</sup> LPS was selected for further experiments. Among all the tested inflammatory markers, this concentration always



revealed a large difference between control and activated cells and was not statistically different from  $500 \text{ ng} \cdot \text{mL}^{-1}$ , which is important for the evaluation if it occurs an inflammatory attenuation by polyphenolic digested fractions.

Additionally, flow cytometry analysis allowed the confirmation of consistent morphological alterations in cells observed at microscope and previously described in the literature as occurring during microglial activation<sup>4,10</sup>. By analyzing forward scatter *versus* side scatter, two physical markers for size and complexity respectively, there is notably a new sub-population that is believed to be activated amoeboid microglia (Figure 8 - B). This microglial sub-population is highly increased in LPS-stimulated microglia, even so it consists of a minority (32.27%) in total analyzed microglia.

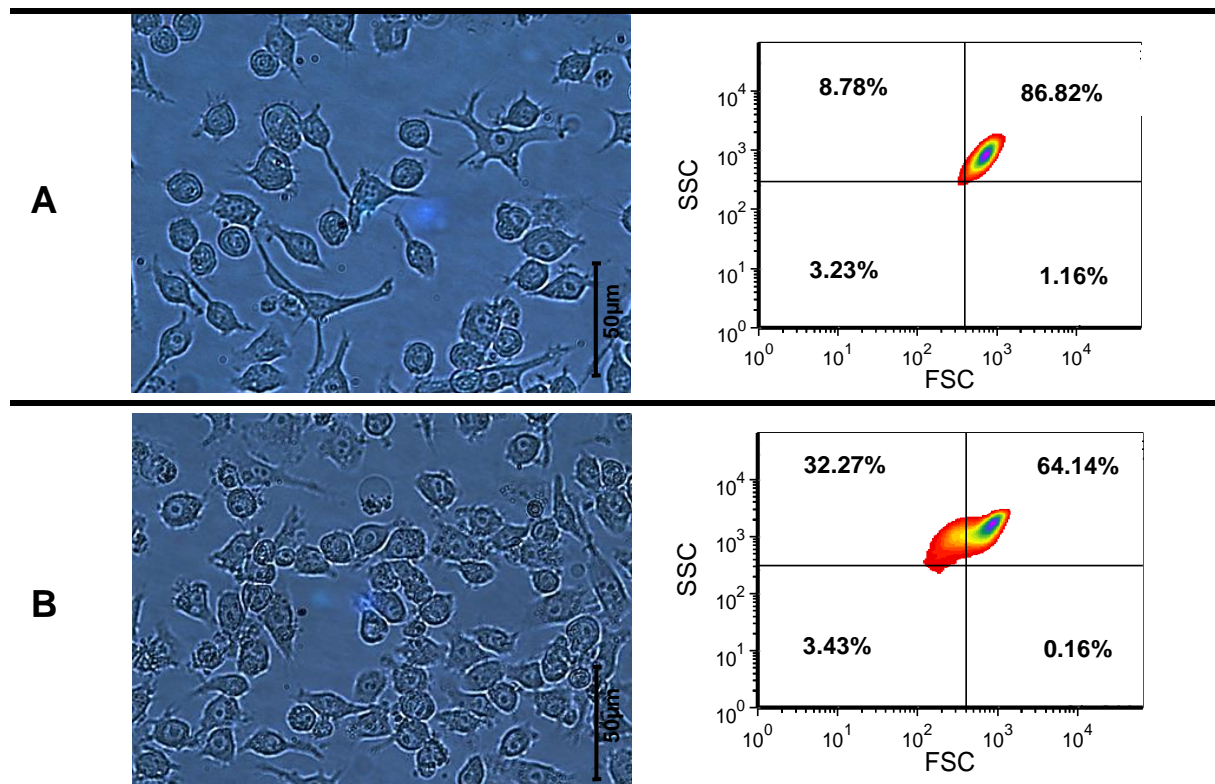


**Figure 8 – (A)** N9 control cells. At left, a microscopy image evidencing cell branches and spaced cellular bodies, typical in non-activated microglia; at right, a flow cytometry density plot demonstrating the unstimulated microglia population with SSC (side scatter) vs FSC (forward scatter). **(B)** N9 cells stimulated with  $300 \text{ ng} \cdot \text{mL}^{-1}$  of LPS. At left, a microscopy image showing activated cells with a modified morphology, retracted processes and segregated vesicles. At right, a flow cytometry density plot evidencing a new sub-population of activated cells.

#### 4.1.2 – Cytotoxicity of the digested raspberry polyphenolic fractions

The cytotoxicity assay did not show significant differences among the five digested raspberry fractions, independently of the concentration tested (Figure 9). This means that each fraction at any of the concentrations tested, has no significant cytotoxic effects. However, for the following experiments, only one concentration ( $1 \text{ } \mu\text{g GAE} \cdot \text{mL}^{-1}$ ) was chosen to test the

anti-inflammatory capacity, since it is closer to the described physiological levels of polyphenols in blood<sup>143</sup>.

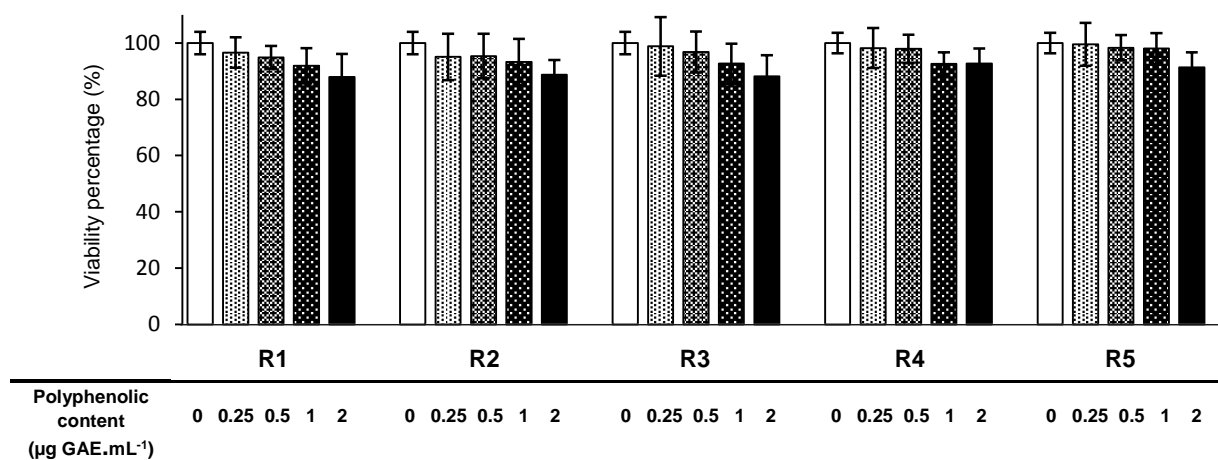


**Figure 9** - Cytotoxicity of the digested raspberry fractions in N9 microglial cells. Results were obtained with CellTiter-Blue cell viability assay and are representative of three biological replicates with  $\pm$  SE. No significant differences were found.

#### 4.1.3 – Model optimization for attenuation of neuroinflammation

To implement a model that could be used to study the effect of the different digested raspberry fractions on the attenuation of neuroinflammation, an assay to identify the best incubation time was performed. Due to the limited amount of the digested raspberry fractions under study, a different but similar digested raspberry fraction was used in this assay (“HT” - Himbo Top digested raspberry polyphenolic fraction), previously tested at host laboratory with some evidence in attenuating neuroinflammation (unpublished data).

For this assay, different times of pre-incubation with HT ( $1.25 \mu\text{g GAE} \cdot \text{mL}^{-1}$ ) were tested in LPS-stimulated cells ( $300 \text{ ng} \cdot \text{mL}^{-1}$ ; 24h), accordingly to literature<sup>105, 144</sup>. The release of NO and TNF- $\alpha$ , was evaluated, as seen in Table 5. Clearly, when comparing the percentage of inflammatory attenuation in both inflammatory markers for each different incubation time, it was decided to further utilize incubations with 6 hours, since it is the timeframe where the major attenuation was detected.

**Table 5** – Percentage of inflammatory attenuation, quantified by released NO and TNF- $\alpha$ , both obtained from cells incubated with HT fraction ( $1.25 \mu\text{g GAE} \cdot \text{mL}^{-1}$ ) during 2h; 4h; 6h and 24h. Percentages of attenuation and the respective standard errors were obtained by normalization for the respective inflammatory positive controls. Significance data is respective to the difference between inflammatory positive controls and the cells pre-treated with HT. [\*\*\*  $p < 0.001$ ; \*\*  $p < 0.01$ ; \*  $p < 0.05$ ; n.s.  $p > 0.05$  (not statistically significant)].

	% of reduction in NO	% of reduction in TNF- $\alpha$
2h	30.16% $\pm$ 5.35% *	27.66% $\pm$ 1.55% ***
4h	31.74% $\pm$ 2.92% **	34.09% $\pm$ 4.08% *
6h	33.18% $\pm$ 2.35% **	42.52% $\pm$ 4.67% ***
24h	17.73% $\pm$ 1.42% n.s.	7.44% $\pm$ 1.03% n.s.

#### 4.1.4 – Attenuation of neuroinflammation by raspberry digested fractions

After the model optimization, the potential to attenuate the neuroinflammation by the five digested quasi-isogenic raspberry polyphenolic fractions (R1, R2, R3, R4 and R5) was assayed. The microglial pro-inflammatory markers NO, TNF- $\alpha$ , CD-40 and O<sub>2</sub><sup>-</sup> were quantified after pre-treatment with the digested fractions, followed by LPS stimulation.

In respect to NO measurement, pre-treatments with all the digested fractions significantly decreased the secretion of this pro-inflammatory mediator by N9 microglial cells, relatively to inflammatory positive control (Figure 10 – A). Regarding TNF- $\alpha$  quantification, only the digested fractions R1, R2 and R5 had significantly reduced the secretion of this cytokine (Figure 10 – B). R5 was the digested fraction that most reduced the release of both markers, NO and TNF- $\alpha$ .

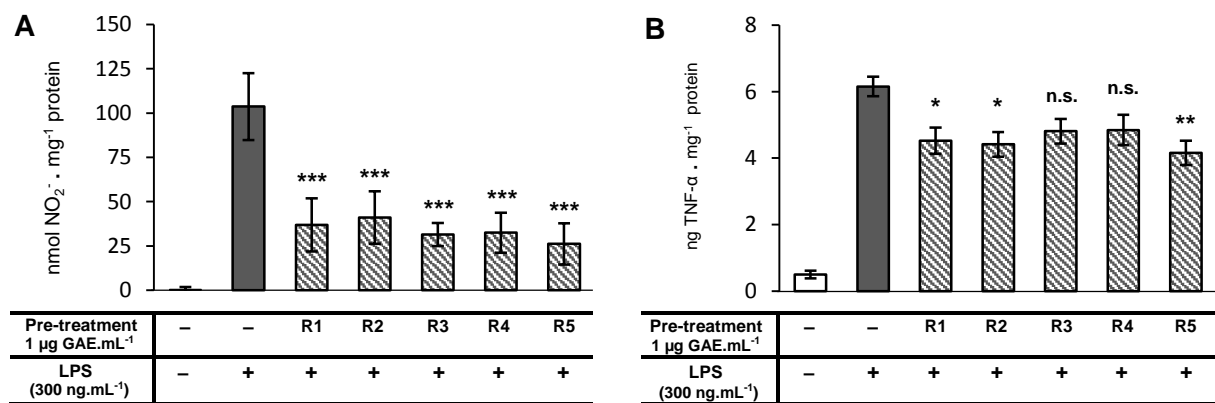


**Figure 10** – Cells were pre-treated with 1  $\mu\text{g GAE} \cdot \text{mL}^{-1}$  of the five raspberry fractions for 6 hours before inflammatory stimulation with LPS for 24h. (A) Quantification of the released NO by N9 microglial cells, using Griess reaction; (B) quantification of released TNF- $\alpha$  by N9 microglial cells, using quantitative ELISA. Both results were normalized for the extracted protein in each treatment with  $\pm$  SE. Solid white bars represent the cells with no pre-treatment and no LPS stimulation (inflammatory negative control); Solid grey bars represent cells with no pre-treatment but with LPS stimulation (inflammatory positive control); Striped bars represent the cells pre-treated with the different fractions before LPS stimulation. Statistical data is respective to the differences between each pre-treatment (striped bars) and the control (solid fill bars). [\*\*\*  $p < 0.001$ ; \*\*  $p < 0.01$ ; \*  $p < 0.05$ ; n.s.  $p \geq 0.05$  (not statistically significant)].

Relatively to the quantification of CD-40 expressed by N9 cells, a significant attenuation in the percentage of cells highly expressing this marker was verified when pre-treated with any of the tested raspberry digested fractions (R1, R2, R3, R4 and R5) (Figure 11 - A). Even so, R3 and R4 exhibited a lower reduction in the percentage of cells highly expressing CD-40, compared to R1, R2 and R5 digested fractions. Additionally, R5 was the digested fraction that most attenuated the percentage of N9 cells highly expressing CD-40, by reaching 34.73%, which is near the non-stimulated cells (20.95%).

Quantification of superoxide in N9 cells also revealed a significant reduction in the production of this marker by cells pre-treated with some of the digested fractions, comparing to the positive control (Figure 11 - B). Only pre-treatments with R3 and R4 fractions had no significant attenuation in superoxide production. However, from the significant attenuations

promoted by R1, R2 and R5 fractions, the R5 was the most accentuated by nearing the control levels.

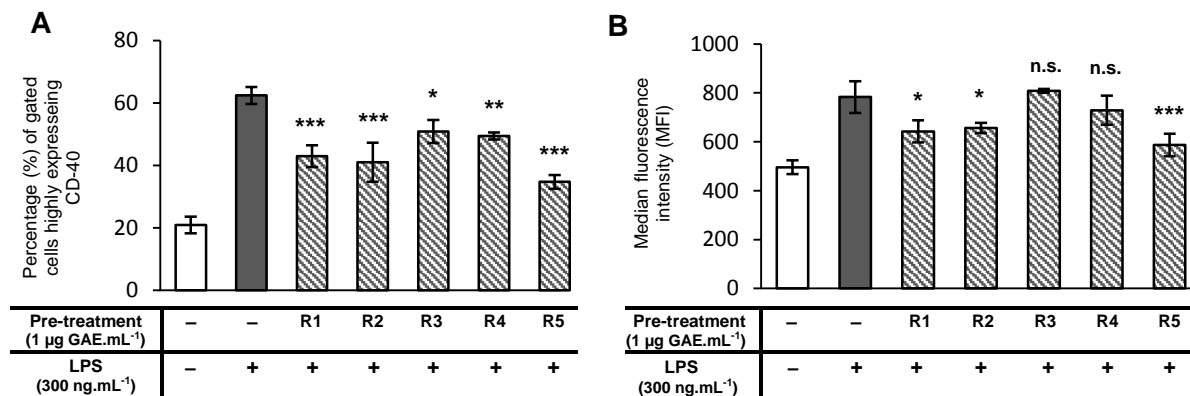


**Figure 11** – Expression of CD-40 and production of intracellular  $O_2^-$  both quantified by flow cytometry analysis of stained N9 microglial cells pre-incubated with  $1 \mu\text{g GAE} \cdot \text{mL}^{-1}$  of each digested fraction before pro-inflammatory stimulation with  $300 \text{ ng} \cdot \text{mL}^{-1}$  LPS for 24h. **(A)** Quantification of the percentage of gated cells that highly express CD-40. **(B)** Quantification of intracellular  $O_2^-$  production by median fluorescence intensity (MFI). Solid white bars represent the cells with no pre-treatment with fraction and no LPS stimulation (inflammatory negative control); Solid grey bars represent cells with no pre-treatment but with LPS stimulation (inflammatory positive control); Striped bars represent the cells pre-treated with the different fractions before LPS stimulation. Statistics are representative of 3 biological replicates with  $\pm$  SD. \* represent statistical significance relative to inflammatory positive controls (solid gray bars). [\*\*\*  $p < 0.001$ ; \*\*  $p < 0.01$ ; \*  $p < 0.05$ ; n.s.  $p \geq 0.05$  (not statistically significant)].

Together, these results clearly demonstrate that the five digested raspberry polyphenolic fractions act differently as inflammatory attenuators in LPS-stimulated N9 cells. The pre-treatments with R3 and R4 fractions clearly evidence a lower capacity in attenuating neuroinflammation, since for the  $\text{TNF-}\alpha$  and  $O_2^-$  measurements, no significant decrease in both pro-inflammatory markers was found relatively to the inflammatory positive controls (Figure 10 - B and Figure 11 - B), respectively. In addition, the percentage of cells highly expressing CD-40 was not as reduced with R3 and R4, as it was with R1, R2 and R5 pre-treatments (Figure 11 - A).

Oppositely, R1, R2 and R5 pre-treatments significantly reduced the secretion of NO and  $\text{TNF-}\alpha$ , as well as the production of  $O_2^-$ , and the expression of CD-40, in LPS-stimulated cells. Nevertheless, the R5 fraction stands out, considering that, on average it has decreased every microglial inflammatory marker more than all the other digested fractions did, suggesting its strong contribution for the attenuation of neuroinflammation in general.

## 4.2. Mechanistic studies of anti-inflammatory properties of digested raspberry polyphenols in *Saccharomyces cerevisiae* models

Yeasts are still the most worthwhile organism for studying the relationship between genotype and phenotype in eukaryotic cells<sup>145</sup>. Expression of heterologous proteins in yeast cells can facilitate the connection between structure and function in other organisms. This strongly validates the use of yeasts as models for primary deduction of functional and mechanistic aspects of protein systems shared by eukaryotes<sup>146</sup>.

### 4.2.1 – Digested raspberry polyphenols modulate the *Crz1*/calcineurin pathway

A *S. cerevisiae* model of inflammation was used to give insights on the molecular mechanisms behind the attenuation of inflammation observed for the different digested raspberry polyphenol fractions. The model recapitulates the induction of Ca<sup>2+</sup>-signaling cascades leading to the activation of pro-inflammatory genes. Crz1, the yeast orthologue of the mammalian NFAT, mediates this activation in *S. cerevisiae*. For the evaluation of anti-inflammatory activity of digested raspberry polyphenol fractions, two different assays, both using the variations in  $\beta$ -galactosidase activity as reporter to infer Crz1 activation, were used. The *Crz1*/calcineurin pathway was induced with MnCl<sub>2</sub><sup>139</sup>.

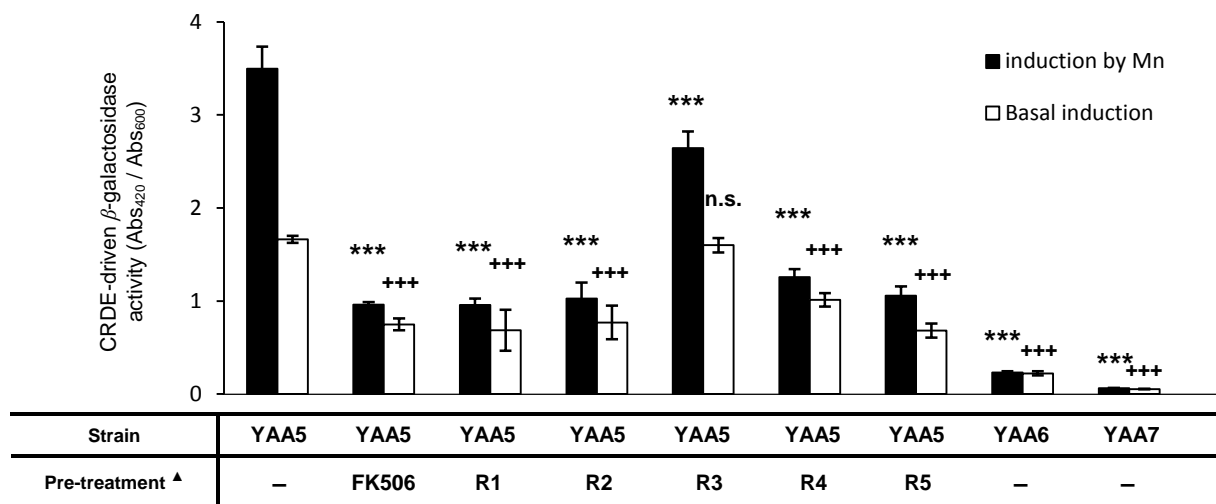
In the qualitative assay, using X-Gal (see chapter 3.3.2), all the fractions reduced the  $\beta$ -galactosidase activity relatively to the control (Table 6). As in the microglia, the digested fractions R2 and R5 presented the strongest effect, apparently higher than the FK506 immunosuppressant. In contrast, R1 and R3 were the digested fractions with the lower inhibitory capacity. YAA6 and YAA7 strains, the negative controls, where the Ca<sup>2+</sup>-signaling cascades are disrupted by the deletion of *CRZ1* and *CNB1* respectively, did not exhibit detectable  $\beta$ -galactosidase activity, as expected.

**Table 6** – Monitoring of  $\beta$ -galactosidase activity in solid medium using XGgal as a chromogenic substrate. *S. cerevisiae* cells were spotted onto agar plates supplemented with 1.8mM MnCl<sub>2</sub> and overlaid with Top-agar containing X-Gal. The development of blue color was recorded 50 minutes after overlay casting. On the top line are represented the strains and respective treatments used.

	YAA5 Control	YAA5 FK506 6 $\mu\text{g.mL}^{-1}$	YAA5 R1 100 $\mu\text{g.mL}^{-1}$	YAA5 R2 100 $\mu\text{g.mL}^{-1}$	YAA5 R3 100 $\mu\text{g.mL}^{-1}$	YAA5 R4 100 $\mu\text{g.mL}^{-1}$	YAA5 R5 100 $\mu\text{g.mL}^{-1}$	YAA6 $\Delta\text{CRZ1}$ control	YAA7 $\Delta\text{CNB1}$ control
MnCl <sub>2</sub> (1.8 mM)									

Attempting to achieve accurate quantitative results,  $\beta$ -galactosidase activity was measured in liquid yeast cultures using ONPG (see chapter 3.3.2). This assay demonstrated that pre-treatment with all the fractions remarkably inhibited the activity of  $\beta$ -galactosidase relatively to YAA5 control cells induced with 1.8 mM  $MnCl_2$  (Figure 12 – black bars). R3 digested fraction exhibited, by far, the lowest capacity to attenuate  $\beta$ -galactosidase activity, consistent with the previous results.

Regarding the analysis of uninduced cells (Figure 12 – white bars), it is clear a basal  $\beta$ -galactosidase activity, which was also significantly decreased after pre-treatment with the majority of the digested fractions. Indeed, only R3 yielded no significant differences respective to the control. This implies that the majority of fractions not only reduced the  $\beta$ -galactosidase expression induced by  $Mn^{2+}$ , but also decreased the basal activation of Crz1.



<sup>^</sup> - For the immunosuppressant FK506, the concentration used was 6  $\mu g \cdot mL^{-1}$ . For all raspberry digested fractions the concentrations used were 100  $\mu g \text{ GAE} \cdot mL^{-1}$ .

**Figure 12** – Quantitative  $\beta$ -Galactosidase activity levels, quantified by the hydrolysis of ONPG spectrophotometric substrate. Yeast cells were incubated with different pre-treatments, accordingly with the figure. After pre-treatment, each sample was equally separated into 2 samples.  $MnCl_2$  (1.8 mM) was added as inflammatory inducer to the first sample (**solid black bars**); no inflammatory inducer was added to the second sample (**white solid bars**). Data were obtained from 3 technical replicates and were obtained by reading absorbance at 420nm before normalization for the  $Abs_{600}$ . Values are presented in mean  $\pm$  SD. Statistics are relative to the respective control bars (YAA5 with no pre-treatment). \* and + represent statistical significance relative to cells induced by Mn and not induced cells, respectively [\*\*\* and +++  $p < 0.001$ ; n.s.  $p \geq 0.05$  (not statistically significant)].

## 5. Conclusions and future perspectives

This study provided evidence that some digested raspberry polyphenol fractions obtained from the five different quasi-isogenic raspberry cultivars strongly attenuate the expression/production of diverse neuroinflammatory markers in LPS-stimulated microglia. This effect was consistently verified in murine microglial N9 cells, for the pro-inflammatory markers CD-40, NO, O<sub>2</sub><sup>-</sup> and TNF-α after treatments with R1, R2, and especially R5 fractions (Table 7). However, R3 and R4 fractions demonstrated lower capacity in attenuating some of the tested pro-inflammatory markers.

**Table 7** – Final qualitative comparison between the five digested raspberry fractions (R1, R2, R3, R4, R5), regarding the results obtained for each different marker in murine microglial N9 cells and the results achieved with the yeast model of inflammation. Symbols represent the capacity of each fraction in the attenuation of the respective inflammatory marker/technique +++ high capacity; ++ good capacity; + some capacity; 0 no capacity.

Extract	Marker	N9 microglial neuroinflammatory model				Yeast model of inflammation	
		NO	TNF-α	O <sub>2</sub> <sup>-</sup>	CD-40	Qualitative	Quantitative
R1		+++	++	++	++	++	+++
R2		+++	++	++	++	+++	+++
R3		+++	+	0	+	+	+
R4		+++	+	0	+	++	+++
R5		+++	+++	+++	+++	+++	+++

Also, the reduction evidenced in one specific pro-inflammatory marker by one of the digested fractions do not means that the remaining markers follow exactly the same tendency. As example, all fractions greatly reduced NO release by LPS-stimulated microglia, even so, only R1, R2 and R5 significantly reduced TNF-α release and superoxide production. These variations are expected because each quasi-isogenic raspberry has a complex and different polyphenolic constitution (Attachment 2), which can differentially interact with the several pathways involved in the expression/production of each pro-inflammatory marker. This also justifies the use of several markers to assess the anti-inflammatory capacity of compounds.

Although not critical, ongoing work is being developed with Iba-1, to accurately monitor variations in this reliable microglial activation marker. However, as elucidated by the flow cytometry results (Figure 7 Figure 8), not all the LPS-stimulated microglia population become activated. Then, the use of a sorting cytometer would allow the exclusive analysis of the activated microglial population by techniques such as western blot or real-time polymerase chain reaction (qPCR).

Additionally, results obtained using the yeast model strongly suggest that one of the mechanisms by which the digested raspberry polyphenolic fractions attenuate

neuroinflammation in microglia is through the repression of Ca<sup>2+</sup>-signaling pathways, and consequently the pro-inflammatory gene expression driven by NFAT. As previously referred, this is a key pathway that regulate the microglial activation by the secretion of pro-inflammatory cytokines such as TNF- $\alpha$ <sup>27</sup>. The use of the yeast model also strengthened R1, R2 and R5 as the fractions with higher potential to attenuate neuroinflammation. Conversely, the R3 fraction was confirmed to be the fraction with the lowest anti-inflammatory power.

With the comparison between the results obtained with all the digested fractions and their chemical characterization, important aspects were highlighted. Firstly, the capacity in attenuating neuroinflammation does not seem to depend on the total phenols content. Additionally, two of the fractions that evidenced higher neuroinflammatory attenuation (R2 and R5) have the lowest concentrations, by far, in total flavonoids and anthocyanins. However, these fractions have relatively high concentrations in total ellagic acid conjugates.

Ellagic acid and its conjugates may have a beneficial role in the attenuation of neuroinflammation<sup>147, 148</sup>. The opposite was demonstrated in the present work relatively to the anthocyanin content, since the fraction with the higher anthocyanin content (R4) exhibited low capacity to attenuate neuroinflammation. Moreover, R5 – the yellow raspberry, with nearly no anthocyanin content, strongly attenuated all the tested pro-inflammatory activation markers in microglia, as well as Crz1 activation in the yeast model of inflammation. Nevertheless, the synergistic effect can also be the key for the anti-inflammatory capacity promoted by these fractions, and not only the composition in a restrict group of polyphenols.

Not less important is the fact that this study has been carried out with digested fractions produced by an *in vitro* digestion model, which is not always possible in similar studies. It is also important to emphasize the fact that the digested fractions were used at concentrations near the physiologic levels found in blood serum, accordingly with literature<sup>143</sup>.

In the future, these fractions should be tested in other neuroinflammatory models, such as human microglia cell lines or primary microglial cells. It is equally necessary to understand if any neuroprotective effect also accompanies the neuroinflammatory attenuation promoted by these fractions, and if all together contribute for the prevention / regression of some of the neurodegenerative disorders such as Parkinson's or Alzheimer's diseases.



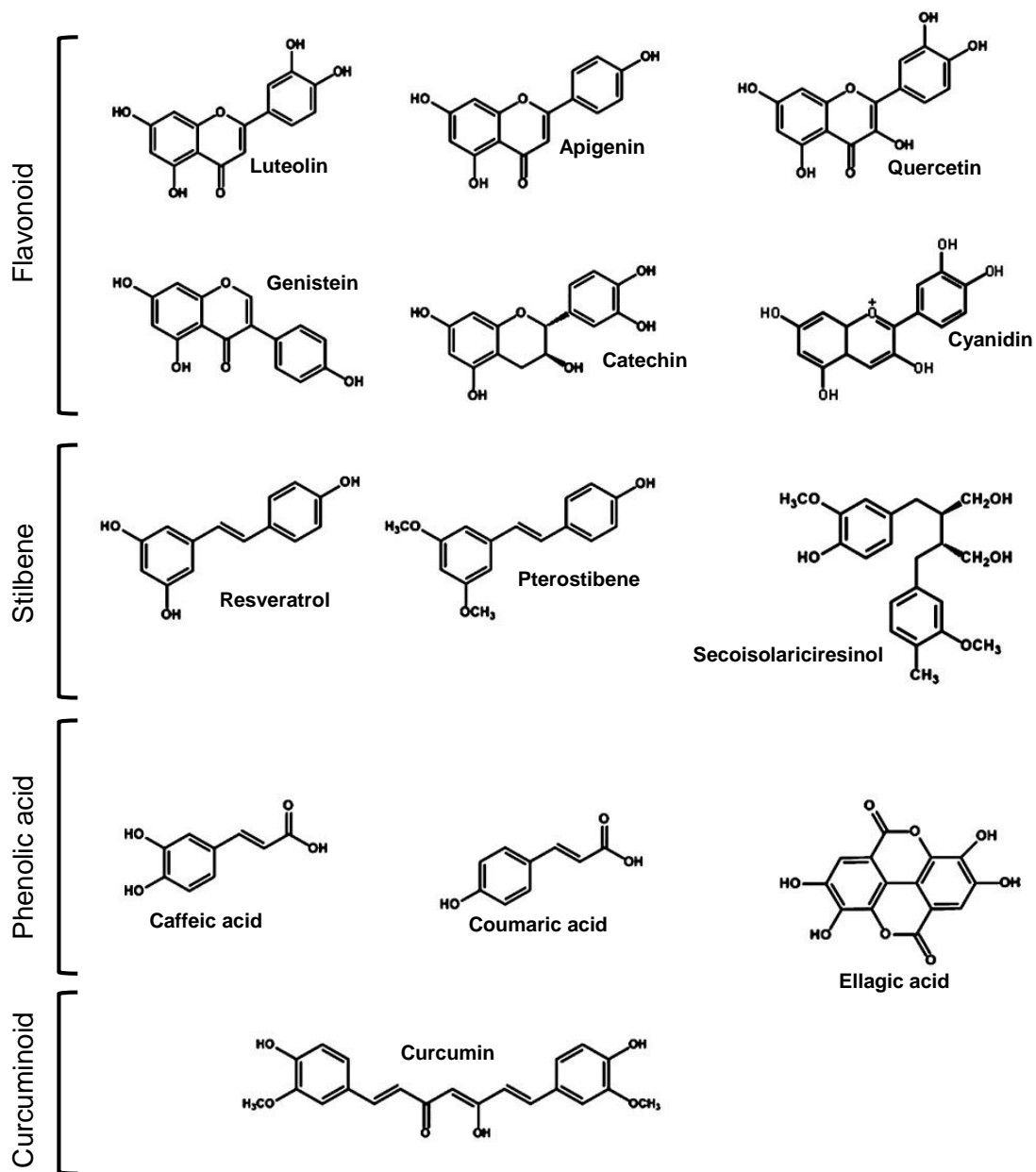
## 6. References

1. H. E. Gendelman, *J Neurovirol* **8**, 474 (2002).
2. P. del Rio-Hortega. (Penfeild Wed, New York, 1932), vol. Penfeild Wed, New York.
3. A. Ghosh, *ANNALS OF NEUROSCIENCES* **17**, 191 (2010).
4. A. Karperien, H. Ahammer, H. F. Jelinek, *Front Cell Neurosci* **7**, 3 (2013).
5. A. Nimmerjahn, F. Kirchhoff, F. Helmchen, *Science* **308**, 1314 (2005).
6. F. Aloisi, *Glia* **36**, 165 (2001).
7. A. D. Dick, A. L. Ford, J. V. Forrester, J. D. Sedgwick, *Br J Ophthalmol* **79**, 834 (1995).
8. H. Akiyama, P. L. McGeer, *J Neuroimmunol* **30**, 81 (1990).
9. R. M. Hoek *et al.*, *Science* **290**, 1768 (2000).
10. G. W. Kreutzberg, *Trends Neurosci* **19**, 312 (1996).
11. M. B. Graeber, W. J. Streit, G. W. Kreutzberg, *J Neurocytol* **17**, 573 (1988).
12. W. Oehmichen, M. Gencic, *Acta Neuropathol Suppl* **Suppl 6**, 285 (1975).
13. M. Sawada, N. Kondo, A. Suzumura, T. Marunouchi, *Brain Res* **491**, 394 (1989).
14. S. C. Lee, W. Liu, D. W. Dickson, C. F. Brosnan, J. W. Berman, *J Immunol* **150**, 2659 (1993).
15. M. Mogi *et al.*, *Neurosci Lett* **165**, 208 (1994).
16. S. T. Dheen, Y. Jun, Z. Yan, S. S. Tay, E. A. Ling, *Glia* **50**, 21 (2005).
17. L. Qin *et al.*, *J Neurochem* **83**, 973 (2002).
18. M. Ii, M. Sunamoto, K. Ohnishi, Y. Ichimori, *Brain Res* **720**, 93 (1996).
19. E. Farkas, G. I. De Jong, R. A. de Vos, E. N. Jansen Steur, P. G. Luiten, *Acta Neuropathol* **100**, 395 (2000).
20. C. T. Ekdahl, Z. Kokaia, O. Lindvall, *Neuroscience* **158**, 1021 (2009).
21. I. Yang, S. J. Han, G. Kaur, C. Crane, A. T. Parsa, *J Clin Neurosci* **17**, 6 (2010).
22. W. J. Streit, *Glia* **40**, 133 (2002).
23. M. G. Tansey, M. K. McCoy, T. C. Frank-Cannon, *Exp Neurol* **208**, 1 (2007).
24. C. L. Willis, *Toxicol Pathol* **39**, 172 (2011).
25. T. C. Frank-Cannon, L. T. Alto, F. E. McAlpine, M. G. Tansey, *Mol Neurodegener* **4**, 47 (2009).
26. A. D. Kraft, G. J. Harry, *Int J Environ Res Public Health* **8**, 2980 (2011).
27. K. Nagamoto-Combs, C. K. Combs, *Journal of Neuroscience* **30**, 9641 (2010).
28. M. L. Block, L. Zecca, J. S. Hong, *Nat Rev Neurosci* **8**, 57 (2007).
29. H. Hu, Z. Li, X. Zhu, R. Lin, L. Chen, *Evid Based Complement Alternat Med* **2014**, 383821 (2014).
30. B. Tian, A. R. Brasier, *Recent Prog Horm Res* **58**, 95 (2003).
31. T. D. Gilmore, *Oncogene* **25**, 6680 (2006).
32. A. E. Frakes *et al.*, *Neuron* **81**, 1009 (2014).
33. G. Courtois, T. D. Gilmore, *Oncogene* **25**, 6831 (2006).
34. M. Karin, *Nature* **441**, 431 (2006).
35. H. Qin, C. A. Wilson, S. J. Lee, X. Zhao, E. N. Benveniste, *Blood* **106**, 3114 (2005).
36. N. S. Chandel, W. C. Trzyna, D. S. McClintock, P. T. Schumacker, *J Immunol* **165**, 1013 (2000).
37. D. C. Fitzgerald *et al.*, *Vet Immunol Immunopathol* **116**, 59 (2007).
38. P. Renard *et al.*, *Biochem Pharmacol* **53**, 149 (1997).
39. M. Karin, Y. Ben-Neriah, *Annu Rev Immunol* **18**, 621 (2000).
40. E. Serfling *et al.*, *Biochim Biophys Acta* **1498**, 1 (2000).
41. A. Rao, C. Luo, P. G. Hogan, *Annu Rev Immunol* **15**, 707 (1997).
42. A. Kiani, A. Rao, J. Aramburu, *Immunity* **12**, 359 (2000).
43. B. Xing, A. D. Bachstetter, L. J. Van Eldik, *Mol Neurodegener* **6**, 84 (2011).
44. S. H. Kim, C. J. Smith, L. J. Van Eldik, *Neurobiol Aging* **25**, 431 (2004).
45. B. M. Babior, *Am J Med* **109**, 33 (2000).
46. M. L. Block, J. S. Hong, *Prog Neurobiol* **76**, 77 (2005).
47. L. Qin *et al.*, *J Biol Chem* **279**, 1415 (2004).
48. S. H. Choi, S. Aid, H. W. Kim, S. H. Jackson, F. Bosetti, *J Neurochem* **120**, 292 (2012).
49. K. J. Barnham, C. L. Masters, A. I. Bush, *Nat Rev Drug Discov* **3**, 205 (2004).
50. G. D. Ross, V. Vetvicka, *Clin Exp Immunol* **92**, 181 (1993).
51. V. Le Cabec, S. Carreno, A. Moisand, C. Bordier, I. Maridonneau-Parini, *J Immunol* **169**, 2003 (2002).
52. X. Hu *et al.*, *J Immunol* **181**, 7194 (2008).
53. O. T. Lynch, M. A. Giembycz, P. J. Barnes, P. G. Hellewell, M. A. Lindsay, *Br J Pharmacol* **128**, 1149 (1999).
54. R. R. Ingalls *et al.*, *Prog Clin Biol Res* **397**, 107 (1998).
55. C. S. McKimmie, J. K. Fazakerley, *J Neuroimmunol* **169**, 116 (2005).
56. S. Akira, S. Uematsu, O. Takeuchi, *Cell* **124**, 783 (2006).
57. C. S. Jack *et al.*, *J Immunol* **175**, 4320 (2005).
58. J. K. Olson, S. D. Miller, *J Immunol* **173**, 3916 (2004).
59. E. Lien *et al.*, *J Clin Invest* **105**, 497 (2000).
60. S. Lehnardt *et al.*, *Proc Natl Acad Sci U S A* **100**, 8514 (2003).
61. S. Chakravarty, M. Herkenham, *J Neurosci* **25**, 1788 (2005).

62. M. Bsibsi, R. Ravid, D. Gveric, J. M. van Noort, *J Neuropathol Exp Neurol* **61**, 1013 (2002).
63. L. A. Vogel, R. J. Noelle, *Semin Immunol* **10**, 435 (1998).
64. T. F. Pais *et al.*, *EMBO J* **32**, 2603 (2013).
65. K. Rezaei-Zadeh *et al.*, *J Neuroinflammation* **5**, 41 (2008).
66. B. Becher, J. P. Antel, *Glia* **18**, 1 (1996).
67. R. N. Dilger, R. W. Johnson, *J Leukoc Biol* **84**, 932 (2008).
68. A. H. Sprague, R. A. Khalil, *Biochem Pharmacol* **78**, 539 (2009).
69. A. K. Talley *et al.*, *Mol Cell Biol* **15**, 2359 (1995).
70. J. Guadagno, X. Xu, M. Karajgikar, A. Brown, S. P. Cregan, *Cell Death Dis* **4**, e538 (2013).
71. W. Swardfager *et al.*, *Biol Psychiatry* **68**, 930 (2010).
72. R. M. Locksley, N. Killeen, M. J. Lenardo, *Cell* **104**, 487 (2001).
73. W. Droge, *Physiol Rev* **82**, 47 (2002).
74. B. M. Babior, *Blood* **64**, 959 (1984).
75. J. D. Lambeth, *Free Radic Biol Med* **43**, 332 (2007).
76. C. A. Colton, D. L. Gilbert, *FEBS Lett* **223**, 284 (1987).
77. Z. Pei *et al.*, *Glia* **55**, 1362 (2007).
78. V. C. Stewart, S. J. Heales, *Free Radic Biol Med* **34**, 287 (2003).
79. D. W. Moss, T. E. Bates, *Eur J Neurosci* **13**, 529 (2001).
80. Y. Imai, I. Iyata, D. Ito, K. Ohsawa, S. Kohsaka, *Biochem Biophys Res Commun* **224**, 855 (1996).
81. D. Ito, K. Tanaka, S. Suzuki, T. Dembo, Y. Fukuuchi, *Stroke* **32**, 1208 (2001).
82. D. Ito *et al.*, *Brain Res Mol Brain Res* **57**, 1 (1998).
83. I. Boulet *et al.*, *Oncogene* **7**, 703 (1992).
84. N. R. Bhat, P. Zhang, J. C. Lee, E. L. Hogan, *J Neurosci* **18**, 1633 (1998).
85. S. Sanlioglu *et al.*, *J Biol Chem* **276**, 30188 (2001).
86. L. Qin *et al.*, *Glia* **55**, 453 (2007).
87. H. Zhou *et al.*, *Free Radic Biol Med* **52**, 303 (2012).
88. J. Bove, D. Prou, C. Perier, S. Przedborski, *NeuroRx* **2**, 484 (2005).
89. M. Sonia Angeline, P. Chaterjee, K. Anand, R. K. Ambasta, P. Kumar, *Neuroscience* **220**, 291 (2012).
90. X. Wu, A. G. Schauss, *J Agric Food Chem* **60**, 6703 (2012).
91. G. C. Bakker *et al.*, *Am J Clin Nutr* **91**, 1044 (2010).
92. R. C. Masters, A. D. Liese, S. M. Haffner, L. E. Wagenknecht, A. J. Hanley, *J Nutr* **140**, 587 (2010).
93. J. Gonzalez-Gallego, M. V. Garcia-Mediavilla, S. Sanchez-Campos, M. J. Tunon, *Br J Nutr* **104 Suppl 3**, S15 (2010).
94. A. Crozier, I. B. Jaganath, M. N. Clifford, *Nat Prod Rep* **26**, 1001 (2009).
95. I. Rahman, S. K. Biswas, P. A. Kirkham, *Biochem Pharmacol* **72**, 1439 (2006).
96. W. Guo, E. Kong, M. Meydani, *Nutr Cancer* **61**, 807 (2009).
97. A. Garcia-Lafuente, E. Guillaumon, A. Villares, M. A. Rostagno, J. A. Martinez, *Inflamm Res* **58**, 537 (2009).
98. E. J. Calabrese, *Crit Rev Toxicol* **38**, 249 (2008).
99. D. Vauzour, *Oxid Med Cell Longev* **2012**, 914273 (2012).
100. B. Halliwell, *J Neurochem* **97**, 1634 (2006).
101. S. Shin *et al.*, *Journal of the Korean Society for Applied Biological Chemistry* **55**, 669 (2012).
102. H. P. Kim, K. H. Son, H. W. Chang, S. S. Kang, *J Pharmacol Sci* **96**, 229 (2004).
103. H. Lee *et al.*, *FASEB J* **17**, 1943 (2003).
104. H. Cao *et al.*, *J Inflamm (Lond)* **4**, 1 (2007).
105. F. C. Lau, D. F. Bielinski, J. A. Joseph, *J Neurosci Res* **85**, 1010 (2007).
106. R. J. Williams, J. P. Spencer, *Free Radic Biol Med* **52**, 35 (2012).
107. D. E. Ehrhoefler *et al.*, *Nat Struct Mol Biol* **15**, 558 (2008).
108. T. K. Kao *et al.*, *Life Sci* **86**, 315 (2010).
109. V. Sharma *et al.*, *Brain Res Bull* **73**, 55 (2007).
110. G. Bureau, F. Longpre, M. G. Martinoli, *J Neurosci Res* **86**, 403 (2008).
111. A. Y. Abramov *et al.*, *J Neurosci* **25**, 9176 (2005).
112. Y. Steffen, C. Gruber, T. Schewe, H. Sies, *Arch Biochem Biophys* **469**, 209 (2008).
113. J. M. W. Graham, C. Kole, Ed. (2011), pp. 179–196.
114. C. F. J. F. H. Finn, in *Raspberries*, J. F. Hancock, Ed. (2008), pp. 359-392.
115. R. A. Moyer, K. E. Hummer, C. E. Finn, B. Frei, R. E. Wrolstad, *J Agric Food Chem* **50**, 519 (2002).
116. R. C. Pimpao *et al.*, *J Agric Food Chem* **61**, 4053 (2013).
117. A. Z. Tulio, Jr. *et al.*, *J Agric Food Chem* **56**, 1880 (2008).
118. J. M. Tall *et al.*, *Behav Brain Res* **153**, 181 (2004).
119. M. Larrosa *et al.*, *J Nutr Biochem* **21**, 717 (2010).
120. M. Shukla, K. Gupta, Z. Rasheed, K. A. Khan, T. M. Haqqi, *Nutrition* **24**, 733 (2008).
121. N. P. Seeram, R. A. Momin, M. G. Nair, L. D. Bourquin, *Phytomedicine* **8**, 362 (2001).
122. D. Jean-Gilles *et al.*, *J Agric Food Chem* **60**, 5755 (2012).
123. G. J. McDougall, P. Dobson, P. Smith, A. Blake, D. Stewart, *J Agric Food Chem* **53**, 5896 (2005).
124. L. I. Tavares *et al.*, *Food Chemistry* **131**, 1443 (2011).
125. O. H. Lowry, N. J. Rosebrough, A. L. Farr, R. J. Randall, *J Biol Chem* **193**, 265 (1951).
126. L. C. Green *et al.*, *Anal Biochem* **126**, 131 (1982).
127. M. B. Grisham, G. G. Johnson, J. R. Lancaster, Jr., *Methods Enzymol* **268**, 237 (1996).

128. R. T. Figueiredo *et al.*, *J Biol Chem* **285**, 40714 (2010).
129. J. L. Clements, S. A. John, L. A. Garrett-Sinha, *J Immunol* **177**, 905 (2006).
130. J. O'Brien, I. Wilson, T. Orton, F. Pognan, *Eur J Biochem* **267**, 5421 (2000).
131. B. A. Premack, P. Gardner, *Am J Physiol* **263**, C1119 (1992).
132. A. Stathopoulos-Gerontides, J. J. Guo, M. S. Cyert, *Genes Dev* **13**, 798 (1999).
133. D. P. Matheos, T. J. Kingsbury, U. S. Ahsan, K. W. Cunningham, *Genes Dev* **11**, 3445 (1997).
134. H. K. Rudolph *et al.*, *Cell* **58**, 133 (1989).
135. K. W. Cunningham, G. R. Fink, *J Cell Biol* **124**, 351 (1994).
136. R. T. Ferreira *et al.*, *Microbiology* **158**, 2293 (2012).
137. M. S. Cyert, J. Thorner, *Mol Cell Biol* **12**, 3460 (1992).
138. K. S. Kaleka, A. N. Petersen, M. A. Florence, N. Z. Gerges, *J Vis Exp*, (2012).
139. A. M. Stathopoulos, M. S. Cyert, *Genes Dev* **11**, 3432 (1997).
140. F. Aloisi, R. De Simone, S. Columba-Cabezas, G. Penna, L. Adorini, *J Immunol* **164**, 1705 (2000).
141. B. P. Lockhart, K. C. Cressey, J. M. Lepagnol, *Br J Pharmacol* **123**, 879 (1998).
142. F. O. Dimayuga *et al.*, *J Neuroimmunol* **182**, 89 (2007).
143. C. Manach, G. Williamson, C. Morand, A. Scalbert, C. Remesy, *Am J Clin Nutr* **81**, 230S (2005).
144. R. Foresti *et al.*, *Pharmacol Res* **76**, 132 (2013).
145. D. Botstein, G. R. Fink, *Genetics* **189**, 695 (2011).
146. D. Botstein, G. R. Fink, *Science* **240**, 1439 (1988).
147. D. Cornelio Favarin *et al.*, *Mediators Inflamm* **2013**, 164202 (2013).
148. S. Srigopalram *et al.*, *Appl Biochem Biotechnol* **173**, 2254 (2014).

# Attachments



**Attachment 1-** Structures of major dietary polyphenols and the respective groups

Cultivar	Total phenols (mg.100g <sup>-1</sup> FDW)	Total anthocyanins (LC-PDA) (mg.100g <sup>-1</sup> FDW)	Total flavonols (mg.100g <sup>-1</sup> FDW) (from MS each peak)	Total ellagic acid conj. (relative) (from MS each peak)	Total ellagitannins (relative)
R1 (Glen Enrich IN)	9602	596	13	20	2.4
R2 (0304F6 IN)	3392	151	5	16	1.0
R3 (00123A7 IN)	4412	323	28	12	1.3
R4 (Tulameen IN)	5270	681	21	20	1.4
R5 (2J19 yellow raspberry IN)	5851	3	8	18	1.6

**Attachment 2** – Table with the constitution in polyphenols found in each of the five quasi-isogenic raspberry cultivars.